Understanding Transgene Silencing and Environmental Stress Adaptability in *Chlamydomonas reinhardtii*

By

Bernardo Guzman

A thesis submitted to the Johns Hopkins University in conformity with the requirements for the degree of Masters of Science in Engineering

Baltimore, Maryland

December 2013

Abstract

Microalgae are photosynthetic organisms that can be used as a biofuel source. Their high lipid content and fast growth rate provide an excellent platform for lipid extraction. With the unicellular organism *Chlamydomonas reinhardtii's* genome sequenced, there is the potential for genetically engineering microalgae as a biofuel crop. One challenge for growing algae outdoors is battling with environmental stresses, which includes salt, temperature, heat, and light stress. The addition of these stresses leads to a decrease in cell density and cell viability.

To aid in increasing cell viability and stress tolerance, the anti-apoptotic protein Bcl-x_L has been fused to the yellow fluorescent protein Venus and transformed into *C. reinhardtii*. However, transgene silencing prevents high Bcl-x_L protein expression within the cell. In order to increase expression, it is important to understand how transgenes are silenced and what can be done to improve expression. The Foot and Mouth Disease Virus (FMDV) 2A peptide sequence has been found to increase transgene expression in *C. reinhardtii*. The 2A sequence was used in conjunction with the Venus-Bcl-x_L sequence to develop a new plasmid, pBG. This plasmid was transformed into *C. reinhardtii* and stressed with a high salt concentration (150mM or 250mM NaCl) or photooxidative stress (2μM or 10μM Rose Bengal). The addition of the 2A peptide sequence increased the consistency of Bcl-x_L expression as the pBG cell line was found to maintain high cell viability when compared to other stressed cell lines.

Advisor
Dr. Michael Betenbaugh
Professor, Department of Chemical and Biomolecular Engineering

Julian Rosenberg
Senior Scientist, Synaptic Research

Reader
Dr. Mark Donohue
Professor, Department of Chemical and Biomolecular Engineering

Acknowledgements

I would like to thank Professor Betenbaugh for this amazing opportunity and for all of his guidance. Throughout my time in the lab, Professor Betenbaugh helped me understand the importance of being a leader and dedication to the lab. His support has always pushed me to strive in his lab. I would also like to thank Julian Rosenberg for all of his guidance over the last several years. Julian was able to answer every question that I brought to him, and he has helped me understand so much in this lab. Without his help, this project would have hit many more roadblocks along the way. I would like to thank Bojiao and Andrew C. for their guidance in lab. Their help and suggestions allowed me to improve my project and make it what it is today.

Thank you to the algae team: Coral, Christian, Kathleen, MG, Evan, Nico, and Brian for all of their help. These experiments would not have been possible without your assistance in lab. I would also like to thank the mammalian team: Joey, Kelley, Jimmy, Lena, Mark, and Andrew T. for all of their help during this project.

Lastly, this project would not have been completed without the support of my family. Thank you to my parents Drs. Sonia and Nicolas Guzman, as well as my sister Paloma, my brothers Gabriel and Marcelo, and my girlfriend Kara. Your support and love have always pushed me to be my best, and I could never thank you enough.

Table of Contents

List of Figures

List of Tables

Chapter 1: The Current State for Biofuels

On November 15th, 2013, the Environmental Protection Agency (EPA) proposed to reduce the statutory volume for advanced biofuel that could be expected to be available and consumed for 2014 from 2.75 billion gallons, to 2.20 billion gallons [1, 2]. This reduces the proposed percentage standard (ratio of renewable fuel volume to non-renewable gasoline and diesel volume) from 1.62 percent to 1.33 percent. While reducing the statutory volume will help in meeting target requirements, it threatens investments in the advanced biofuel industry [3]. The rise of biofuels as an alternative to crude oil will occur slowly as economic and technological obstacles limit biofuel production. These technological obstacles include overcoming growth limitations, such as nutrient uptake or photosynthetic efficiency, and adapting to environmental insults.

1.1 Microalgae's Role in Biofuel Development

Microalgae are photosynthetic organisms that have recently been examined as a potential biofuel source. Their rapid growth rate and ability to grow phototrophically, heterotrophically, or mixotrophically, allows them to reach a high cell density to extract high valued products. When cultivating algae, the most desired products are proteins and carbohydrates for feed, lipids for biofuel production, and carotenoids for supplements. Various species of *Chlorella* are approximately 25% lipids, but under nutrient deprived conditions, are able to increase their lipid content to at least 50% [4].

The current microalgae strains that are understood for high lipid production include *Chlorella vulgaris* and *Chlorella emersonii* under nutrient deficient growth, as well as *Scenedesmus obliqus* under nutrient sufficient conditions [5]. When growing algae, there are four stages to their growth: the initial lag phase, the exponential phase, the stationary phase, and the death phase.

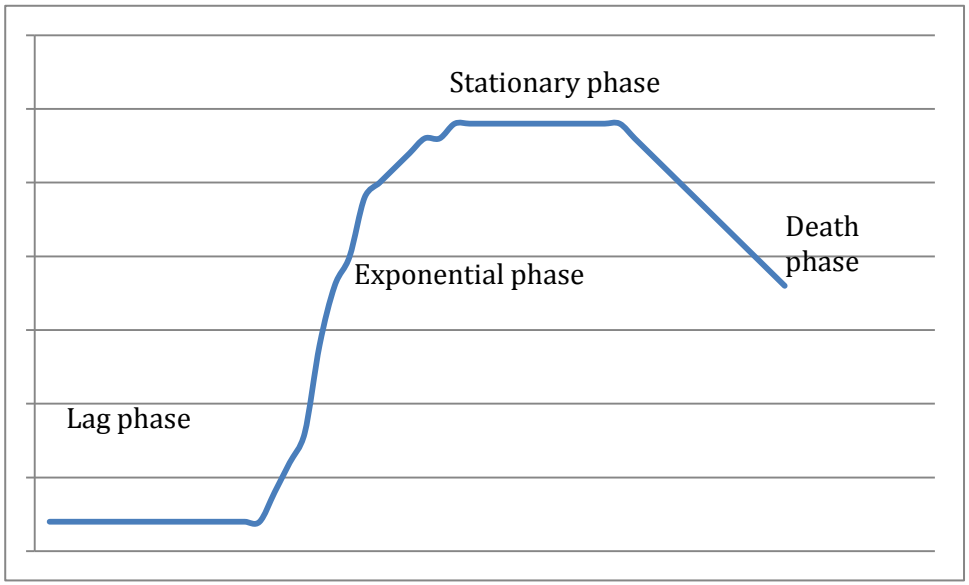

Figure 1 – Example of a cell culture growth curve.

After cell inoculation, the cells adjust to their surroundings. During this time, the cells grow, mature, and slowly start to divide. This is followed by the exponential phase, where most of the cell growth occurs. Cells continue to double until they are constricted by one of several factors: space, nutrients, light, etc. This leads to the stationary phase, where the growth rate is equal to the cell death rate. Lastly, when the cells are out of nutrients, the death rate becomes far greater than the doubling rate, leading to a decrease in cell density.

For biofuel development, the goal is to maintain a high cell density without leading the algae into the death phase. In the case of raceway ponds, fresh media is continuously added to prevent nutrient limitation. In addition to fresh media rich in nitrogen and phosphorus, the addition of CO_2 increases the rate of cell and lipid production [6].

Chapter 2: A Review of Stress Tolerance in Microalgae

2.1 Abiotic Stress Factors

When grown in raceway ponds for high-valued products and lipids, algae react to the shifts in their environment. Abiotic stress responses are important in algae in order to survive under these conditions. The algae's growth is not only limited by nutrients or carbon dioxide, as mentioned previously, but can also be influenced by factors such as salt content, temperature shifts, and light intensity.

2.2 Salt Exposure

While there are many algae species that grow in fresh water, salt exposure limits their growth. In the case of fresh water unavailability, saltwater would be an inadequate replacement because the salt content will prevent algal cell growth. Salt exposure can induce ionic stress, osmotic stress, and oxidative stress [7]. More detail on oxidative stress will appear in Chapter 2.5. With the addition of Sodium Chloride (NaCl) to the cell, there becomes an ion imbalance. The Na^+ ions introduced to the cell compete with Potassium (K^+) ions for cellular uptake. This can not only lead to ion binding sites inhibition, but can also lead to a restricted uptake of water due to the decrease in osmotic potential [8]. The cell must attempt to alleviate any damage done by the salt, reinstate homeostasis, and then resume growth at a reduced rate [9]. Figure 2 shows the signaling pathway when salt is introduced to a cell.

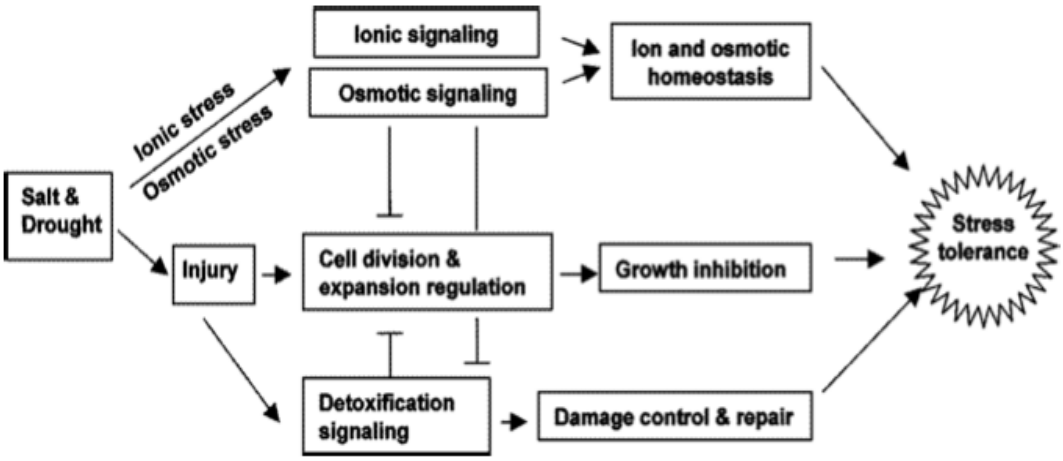

Figure 2 - Salt and Drought Signaling Pathway. Image from Zhu [7]

Salinity and drought effects have been studied within plant cells, but there are few papers published on salt stress response in algae. Salt stress in algae has been recorded to induce several responses. These responses have been collected by Affenzeller et al. and placed in the following table [8]. As seen in the table, *Haematococcus pluvialis* generates the high-valued product astaxanthin as a survival method under stress [17].

Table 1: Algal Response to Salt Stress

Algae Species	Salt Stress Response	Reference
Dunaliella bioculata	Change in ultra-structure	10, Bérubé et al. 1999
Dunaliella tertiolecta	Increase in lipid content and glycerol pool	11, Takagi et al. 2006 12, Goyal 2007
Chlamydomonas reinhardtii	Increase expression of antioxidative enzymes	13, Yoshida et al. 2004
Chlorella zofingiensis	Increase production of astaxanthin	14, Orosa et al. 2001 15, Pelah et al. 2004
Haematococcus pluvialis	Increase production of astaxanthin	14, Orosa et al. 2001 16, Boussiba and Vonshank 1991 17, Boussiba 2000 18, Cordero et al. 1996
Scenedesmus obliquus	Decrease photosynthetic efficiency	19, Demetriou et al. 2007

2.3 Temperature and Heat Stress

Temperatures 10-15°C above ambient temperature are known to induce stress within cells [20]. Allakhverdiev et al. describe the two-step inhibition process of stress-induced impairment. The first step is the direct damage induced by the stress. The second is the generation of reactive oxygen species, which are known for their ability to inhibit protein synthesis. Depending on the severity of the stress and the phase in which the cells are in, the stress may lead to irreparable damage [21].

The algae chloroplast is one of the more sensitive compartments in the cell. Its photosynthetic activity is highly influenced by heat stress [22]. Inside the chloroplast, the photosystems, specifically photosystem II (PSII), are the location of most of the damage caused by heat and salt stress. It is here where stresses for long periods of time will influence the acclimation and the photosynthetic recovery process of the cell [21]. Under

moderate thermal stress, photosynthesis declines. This is due in part by a reduction in the carbon assimilation system and a decline in photosystem activity [21, 23]. In the choloroplast, the thylakoids lose membrane integrity due to the initial heat shock. The thylakoid stack begins to separate, and the carbon assimilation system begins to drop [24, 25]. The elevated temperature reduces the balance of absorbed light between photosystem I and photosystem II [26]. At the same time, high temperatures increase the sensitivity of Rubisco activase, leading to a decline in Rubisco activity [27].

At low temperatures, the D1 protein that is responsible for photosystem repair is inhibited. This is one of the main causes of photoinhibition at low temperatures [28]. But once acclimated to the cold, it is possible for the photosynthetic capacity to recover [28]. This is closely related to the activation of the electron sink process to reduce reactive oxygen species. Additionally, at low temperatures algae have been shown to have increase tolerance to photoinhibitory irradiance [29] due to high photosystem II excitation pressure [30].

2.4 High Light Stress

At high light intensity, the cell's ability to undergo photosynthesis is limited by the quenching of the photosystems, as well as damage to the photochemical reaction center [31]. This can lead to cell damage as photoinhibition occurs, lowering the cell growth rate. When the photosystems are hit with light, the chlorophyll (Chl) antenna reacts according to the intensity. Under low intensity, large Chl antenna are promoted to obtain light. Under high intensity small Chl antenna are promoted to prevent over-excitation of

the photosystems and to prevent potential photo-oxidative damage [31-33]. This is done to prevent over-excitation of the photosystems.

2.5 Oxidative Stress

Oxidative stress occurs through the generation of reactive oxygen species (ROS) such as Hydrogen Peroxide (H_2O_2), singlet oxygen ($^1O_2$), superoxide ion radicals (O_2^-), and hydroxide radicals ($^{\bullet}OH$) [34]. This can be induced by salt, heat, or light stress. The imbalance of ROS in the cell can result in damage to different compartments, specifically the chloroplast since it contains highly energetic reactions for photosynthesis [35]. Induced stress by ROS can lead to lipid hyperperoxidation, membrane damage, and a decrease in overall lipid content for biofuel production [36]. When light energy is supplied at a greater rate than carbon fixation, quenching will occur, leading to ROS generation. But even at low light intensity, the addition of a stress such as salt or heat can affect carbon fixation [17]. When ROS are generated, the cell releases stress proteins and scavenging enzymes to reduce the number of ROS and prevent structural damage [9]. Examples of proteins and enzymes include ascorbate peroxidase (APX), glutathione peroxidase (GPX), and glutathione S-transferase (GST).

2.6 Biotic Stress Factors

While abiotic factors are easy to control experimentally, biotic factors such as pathogens are variable in growth and can interact with other abiotic factors. Examples include members of the genus *Chlorovirus,* which predominantly infect fresh water algae. The

chlorella virus *Parамecium bursaria chlorella virus 1* (PBCV-1) is one of the most studied chlorella viruses to date [37]. The virus' genome is found to be large linear double stranded DNA between 315-380kbp. The virus infects its host by attaching to the external surface of the cell wall [38]. When the virus attaches to the cell wall, it releases a wall digesting enzyme(s) to then fuse the viral DNA with the host's DNA [37]. It has also been recorded that photosynthesis is impaired within 15 minutes of the virus' entry into the algae cell [39]. Moreover, it is inferred that the virus is able to "delete" chloroplast information and possibly reduce the sequence for the D1 protein for photosystem repair. Over time, viral replication will continue until cell lysis occurs.

2.7 Extremophiles and Stress Tolerance

Extremophiles are organisms that survive in extreme conditions, such as low pH, high salinity, and low/high temperature. While most algae are not able to handle extreme conditions, it is possible to analyze current extremophiles and see what allows them to survive in these conditions. The algae can then be engineered with these genes to be able to survive harsher conditions for improved growth. One algal extremophile is *Dunaliella salina,* which is able to survive long periods of time in saturated Sodium Chloride (NaCl). The *Cyanidium caldarium* and *Dunaliella acidophila* can be found in locations with a pH of 0.5 and are known to have high growth at a pH of 1 [40]. These algae are able to survive by maintaining their cytoplasm at a neutral pH, so they will not need to adjust their internal compartment. This can include overexpression of H^+ export enzymes and unique transporters [41].

2.8 Stress-Inducible Genes

Even under abiotic stress conditions, it is possible to take advantage of the cell's survival capabilities. In the case of *Haematococcus pluvialis* under high salt stress, it produces the carotenoid astaxanthin as a survival mechanism. Astaxanthin is a red pigment that contributes to the pink color in shrimp or salmon, and has also been studied for its antioxidant capacity [42]. Under stress, *H. pluvialis* has been recorded to produce astaxanthin up to 4% of the total algal dry weight [43].

When engineering a plasmid, one technique is to incorporate a promoter that activates based on the addition of a stress. The pRelax plasmid will be described later on in more detail, but one key aspect is that it has the HSP70 (Heat Shock Protein 70) promoter. When under heat stress, the promoter is activated and allows for transcription of the following genetic sequence.

2.9 Apoptosis Pathway in Algae

Programmed Cell Death (PCD) is the active process of cell suicide that is induced by both biotic and abiotic stresses. This process is commonly referred to as apoptosis, while the inactive process of cell death is necrosis. Apoptosis is a caspase (cysteine-aspartic protease) cascade that leads to both the shrinking of the cytoplasm, as well as DNA cleavage [44]. When the DNA is cleaved, it is found in multiples of 180bp fragments [45].

The B-cell lymphoma (Bcl) family is a family of proteins that lead the caspase cascade for cell degradation. The Bcl-2 family contains both pro-apoptotic and anti-apoptotic proteins that reside in either the cytosol or in the mitochondria. Pro-apoptotic proteins, like Bax or Bad, induce apoptotic signals in the cytosol culminating in the release of cytochrome c and initiating the pathway. Anti-apoptotic proteins, like Bcl-2 and Bcl-x_L, are mitochondrial transmembrane proteins where they are able to prevent the release of cytochrome c. This is performed by inhibiting mitochondrial pore formation or by maintaining the mitochondria membrane potential [46, 47]. The Bcl-x_L protein has shown to effectively prevent apoptosis within mammalian cell lines, and is not endogenous to algae.

2.10 *Chlamydomonas reinhardtii*: A Model Organism

Chlamydomonas reinhardtii has proven to be the most fruitful microalgal model for genetic transformation. It can grow phototrophically, heterotrophically, or mixotrophically, it has a doubling time of approximately 8 hours, and the microalgae's nuclear genome, as well as its chloroplast and mitochondrial genomes, is publicly available on http://www.phytozome.net/chlamy [48]. Currently, *C. reinhardtii* is one of the only algae strains to allow plasmids to be inserted into the genome. *C. reinhardtii* can be transformed in several ways such as glass beads, electroporation, or particle bombardment, and they require minimal amounts of nutrients when compared to mammalian cell cultures or other plant cultures. There are *C. reinhardtii* species that contain a cell wall, such as UTEX 2244, and there are also mutant strains that survive without a cell wall, such as UTEX 2337.

There have also been several advances in biotechnology due to the research done with *C. reinhardtii*. For RNA interference, it was determined that *C. reinhardtii* does not have a system like those of multicellular organisms, but still contains microRNA (miRNA) for post-transcriptional modifications and monitoring transgene expression [49]. While *C. reinhardtii* does not have the ideal lipid content, 20% under sufficient nutrient conditions, it can serve as a model [5]. As genetic modifications in *C. reinhardtii* are understood, they will eventually be transitioned into the algae strains necessary for high valued products, such as *Chlorella vulgaris* for lipid growth, or *Haematococcus pluvialis* for astaxanthin production.

2.11 Inserting the Bcl-x_L Protein into *C. reinhardtii*

The Bcl-x_L sequence has been codon optimized for the algae *Chlamydomonas reinhardtii* with a fusion to Venus, an enhanced yellow fluorescent protein. Rosenberg et al. transformed *C. reinhardtii* with the Venus-Bcl-x_L fusion sequence along with bleomycin resistance [50]. This plasmid is documented as pRelax. With this plasmid, the lab has demonstrated that the pRelax *C. reinhardtii* cell line is able to resist apoptosis under certain stress conditions. Previous data has shown that while the gene can be found within the genomic DNA, western blots show no protein expression. Between DNA transcription and protein synthesis, there has been low transgene expression. Gene silencing is an issue that can arise between transcription and translation. In order to improve expression, it is important to understand how transgene silencing occurs and what can be done to prevent it.

Chapter 3: Transgene Silencing and Methods to Improve Expression

Gene silencing is the process of restricting transcription of a specific gene within the nucleus. Silencing can be divided into two categories: homology dependent gene silencing and post-transcriptional gene silencing [51]. In homology dependent gene silencing, the host determines that there are numerous copies of related genes. The host then methylates multiple genes resulting in their suppression. Post-transcriptional gene silencing, or RNA interference, can occur when RNA molecules intentionally degrade mRNA. In order to improve transformation efficiency and enhance transgene expression, it is important to understand what methods the cell uses to silence transgenes and how this can be changed.

3.1 Transcriptional Silencing

When DNA tightly coils around a histone, these sequences are silenced. This regulates transcription for the sequences that need to be expressed. The sequences that are not tightly coiled around a histone can be transcribed. Histones can also pack together to form heterochromatin for silencing. Gene transcription has been correlated to high levels of histone acetylation [52], where the addition of acetyl groups to lysine residues loosens the chromatin and allows for transcription [53]. There are two enzymes that are known to regulate histone acetylation, histone acetyltransferase (HAT) and histone deacetyltransferase (HDAC). By increasing the HAT concentration in the cell, it is possible to upregulate gene transcription. RNA polymerase and associated transcription

factors will be able to access the DNA binding sites required for transcription [54]. Likewise, increasing the HDAC concentration would also downregulate transcription and increases the rate of Histone-DNA association. Both HAT and HDAC are targeted to promoters by sequence specific DNA-binding proteins [53]. It has also been determined that histone acetylation levels can return to their normal state after hyperacetylation [55]. In yeast, HATs and HDACs target the entire genome, showing that HATs and HDACs can increase, or decrease, expression of the entire cell [53, 56, 57].

3.2 Regulating Transcriptional Silencing

As mentioned in the previous section, histone acetyltransferases (HATs) and histone deacetyltransferases (HDACs) are specific enzymes that regulate transcription within the nucleus. One method to recognize transcriptionally competent chromatin is the methylation of histone H3 Lys 4 [58]. Methylation of H3K4 can lead to varying degrees of transcription stimulation based on a monomethylated or a trimethylated state [59, 60].

Another method for upregulation of HAT is through the use of Sodium Butyrate. Sodium Butyrate is a salt that can induce hyperacetylation within mammalian cultures [61]. This has been monitored in mammalian cells, but has not been monitored in algae. Additionally, hyperacetlyation can lead to increased global expression in the cell, potentially leading to swelling and cell lysis. Once hyperacetylation occurs, it is possible for the cell to revert back to its normal expression levels either with the removal of the salt, or through adaptation and maintaining ionic and osmotic homeostasis.

A way to enhance transgene expression without regulating HAT/HDAC levels is through the addition of Matrix Attachment Regions (MARs) in the plasmid. Matrix Attachment Regions, also known as Scaffold Attachment Regions (SARs), are sequences ranging from 300-3,000bp, are AT-rich (>65%), contain topoisomerase II sequences, and were previously characterized for their association to the nuclear matrix after the nucleus was treated with detergent [62, 63]. Current estimates suggest that there are at least 50,000 MARs sequences in the mammalian genome [64]. In algae, at least three DNA fragments were found to specifically bind to the nuclear matrix in *D. salina* [65]. While this paper shows promise that there are MARs in algae, this area is limited and needs to be studied further. With an AT-rich sequence, MARs are able to adhere to the matrix, allowing for transcription to occur in sequences between the MARs and the histones.

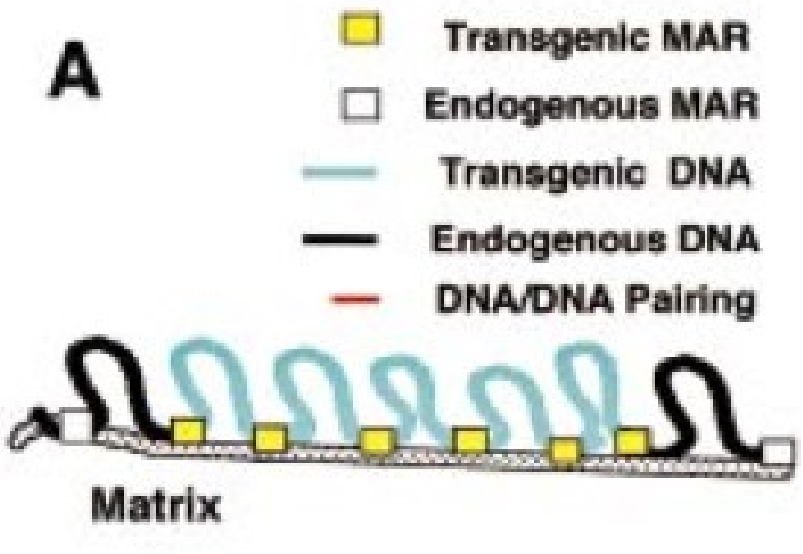

Figure 3 - Matrix Attachment Regions (in yellow) bind to the nuclear matrix, allowing Transgenic DNA (in light blue) to move freely for transcription. Image by Allen et al. [66].

By flanking the gene of interest with MAR sequences, as shown in the figure above, it is possible to expose the transgene for transcription. This will increase transgene expression within the cell. This technique has been popularized in tobacco cells and plants using MAR sequences from chicken and tobacco [67, 68]. The inclusion of MAR sequences flanking a transgene can produce a 60-fold increase in expression level [68].

3.3 Translational Silencing and Regulation

Translational gene silencing is mostly attributed to RNA interference. After the development of mRNA, RNA molecules bind to the mRNA and either degrade it, or allow it to continue its path to protein synthesis. These RNA molecules include

microRNAs (miRNAs) and small interfering RNAs (siRNAs). They regulate gene expression through mRNA cleavage and translational repression [69]. Within *Chlamydomonas reinhardtii*, gene expression has been knocked out via antisense RNAs and dsDNAs. This demonstrates a functional RNA interference system [69, 70]. Moreover, the miRNAs in *C. reinhardtii* have previously cleaved target mRNA [69].

Regulating translational silencing is challenging since there is not much research on RNA interference in algae, specifically *C. reinhardtii*. Articles have been limited to the characterization of different miRNAs, including the sequencing of several small RNAs [71, 49].

3.4 Enhancing Transgene Expression Using the Foot and Mouth Disease Virus (FMDV) 2A Peptide

In a plasmid that contains low transformation efficiency and low expression levels, it can be difficult to monitor or confirm protein synthesis. While it is possible to increase mRNA production through histone modifications or through the use of Matrix Attachment Regions, it is also possible to enhance transgene expression levels using the Foot and Mouth Disease Virus (FMDV) 2A peptide.

The FMDV 2A peptide is approximately 20 amino acids long and is able to self cleave at the last amino acids. During translation elongation, the 2A peptide fails to create a

peptide bond between the final two amino acids. This allows it to self-cleave, with the majority of the 2A peptide sequence attached to the C-terminus of the initial protein. If the 2A peptide sequence is inserted between two protein sequences containing an Open Reading Frame (ORF), then the 2A sequence will be able generate two distinct proteins [72]. This is beneficial for transgene sequences that maintain low expression levels due to silencing. In most cases, the first transgene is an antibiotic resistance (Bleocin, Paramomycin, etc.) and the second is the gene of interest with low expression. The advantage of connecting an antibiotic resistance with the gene of interest via the 2A peptide sequence allows for transformation confirmation by visual observation. If the transformed cell line is able to grow on media containing the antibiotic, then protein of interest expression is expected. However, protein production must be confirmed to ensure no silencing. This has traditionally been done in mammalian and plant cell cultures [73, 74].

Previously, Rasala et al. has increased expression levels of six fluorescent proteins (mCherry, tdTomato, Venus, crGFP, mtagBFP, and mCerulean) using bleomycin resistance and the 2A peptide (ble2A). In this case, the attachment of the fluorescent proteins to ble2A allows for expression throughout the *C. reinhardtii* cell. This was further investigated by fluorescent tagging of the endogenous protein α-tubulin with mCerulean. A mCerulean-α-tubulin fusion sequence was created and led to the fluorescent tagging of the cytoskeleton and flagella where α-tubulin is localized [75]. This shows the ability to increase transgene expression through plasmid development.

3.5 Enhancing Venus-Bcl-x_L Expression in *C. reinhardtii* using the FMDV 2A Peptide

The development and maintenance of the pRelax cell line has proven difficult in the past. With difficulty obtaining a western blot showing protein expression, there is no assurance that the cell line is synthesizing the protein. Colony PCR shows the pRelax plasmid incorporated into the *C. reinhardtii* genomic DNA. With low expression levels, Venus-Bcl-x_L production levels must be increased in one of the methods described above.

This project looks into increasing expression levels through the use of the Foot and Mouth Disease Virus (FMDV) 2A gene to provide consistent transformation efficiency and demonstrate the ability for high Bcl-x_L expression levels. By maintaining the core backbone, bleomycin resistance and the 2A sequence, and coupling this with the Venus-Bcl-x_L fusion sequence, Venus expression can increase within the cell, as well as Bcl-x_L expression on the mitochondria's membrane. With an algae cell line that maintains high anti-apoptotic protein production, the project will look into the effects of several different abiotic stresses on cell viability and adaptability.

3.6 Control and Biocontainment of Genetically Modified Algae

As a platform, *C. reinhardtii* can receive different genes and incorporate them into its genomic DNA. With the background of incorporating non-native genes into algae, it is

important to look at the risks that can develop if algae are released into the wild. A long-term goal for developing commercial biofuels is to re-engineer the algae, either through enhanced lipid production, secreting biofuel feedstocks, enhanced nutrient uptake or photosynthetic efficiency, or stress tolerance. This can be done by altering an existing gene or by inserting a sequence from another organism [76]. By genetically modifying the algae, it must be regulated by the U.S. Environmental Protection Agency as well as the U.S. Department of Agriculture [76].

There are two main ways to contain genetically modified algae and prevent their survival in the environment. One method is to impair the algae cell's ability to transfer genes either sexually or asexually. The second is to add an apoptosis-inducing gene that can be activated when the algae is in a new environment. There is currently a patent on biocontainment of genetically modified algae, where the algae is given a lethal gene that is linked with an inactive promoter in the presence of a repressor compound found in the growth media [77]. The inactive promoter will only be activated when the repressor compound is no longer available, i.e. in the environment. In this case, the algae will only be able to survive in an artificial environment containing the specific repressor compound.

Chapter 4: Genetic Transformation of Chlamydomonas reinhardtii with the FMDV 2A Gene and the Bcl-xL Gene

4.1 Genetic Transformation of *C. reinhardtii* with the Venus-Bcl-x_L Fusion Gene

The *Chlamydomonas reinhardtii* cell line UTEX 2244, obtained from the Culture Collection of Algae at the University of Texas, has been used in the past as a source for algal transformations. The fused genetic sequence known as Venus-Bcl-x_L was developed and provided by Julian Rosenberg [50]. The Venus-Bcl-x_L sequence is codon optimized for algae, and was previously transformed into *C. reinhardtii* creating the cell line known as pRelax. The pRelax cell line also contains the genetic sequence for bleomycin resistance (ble) as well as the Heat Shock Protein 70 (HSP70) promoter, which helps in initiating transcription of the plasmid.

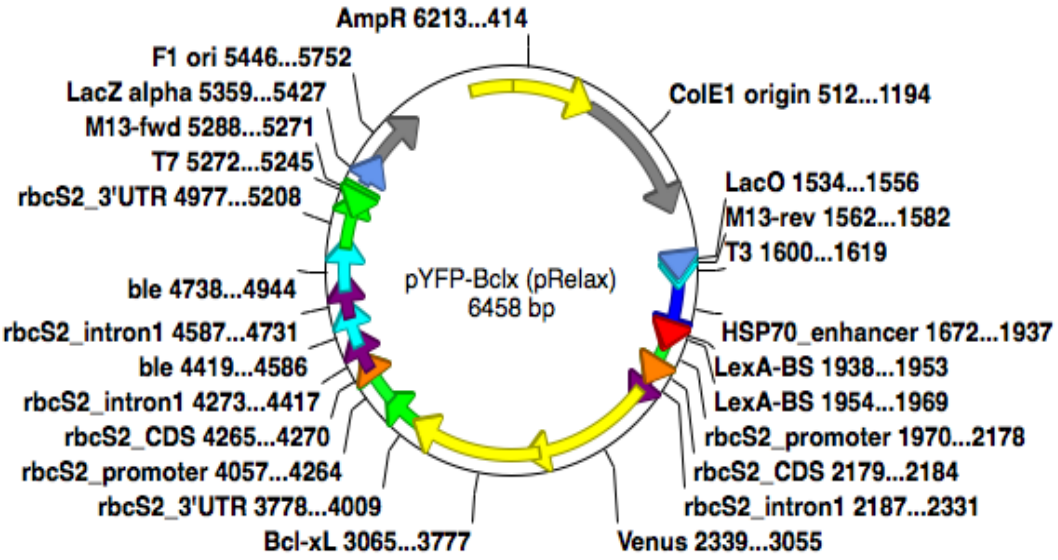

Figure 4 - pRelax Plasmid Map

4.2 Genetic Transformation of *C. reinhardtii* with the FMDV 2A Peptide Gene

The Foot and Mouth Disease Virus (FMDV) 2A gene was provided by Beth Rasala from the University of California, San Diego in two plasmids: pBR9 and pBR25. The plasmid pBR9 contains the genes encoding for bleomycin resistance (ble), the FMDV 2A peptide, and GFP. The pBR25 plasmid contains the genes encoding for bleomycin resistance, the FMDV 2A peptide, mCerulean, and α-tubulin. Both plasmids have been previously published [72, 75]. Beth Rasala also contributed *C. reinhardtii* cells containing pBR9-Venus (YFP replacing GFP) for additional experimentation.

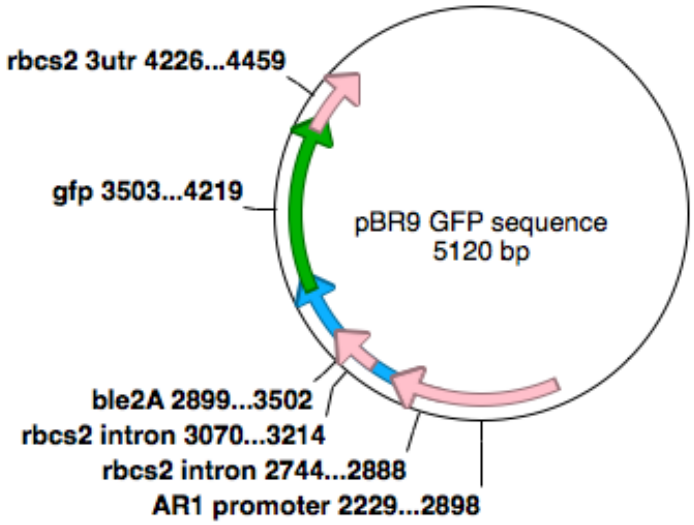

Figure 5 - pBR9 Plasmid Map. Image obtained from the ApE sequence provided by Beth Rasala.

4.3 pBG Formation – The Synthesis of the FMDV 2A Sequence and Venus-Bcl-x_L

The pBR9 plasmid, ble2A-GFP, was transformed in chemically competent *E. coli* cells and incubated in a 37°C shaker overnight. The cells were then transferred to an LB plate with 20µl Ampicillin (1000x) and allowed to incubate at 37°C until colonies formed. Colonies were selected, grown overnight, and a QIAprep Spin Miniprep kit was used to isolate the plasmid DNA. 2µg of the harvested DNA was digested with BamHI-HF and XhoI restriction enzymes overnight and placed in an agarose gel for gel electrophoresis. The result was the pBR9 backbone, containing bleomycin resistance and the FMDV 2A linker, separated from the 717bp GFP sequence. The backbone was removed from the gel using a QIAgen Gel Purification kit.

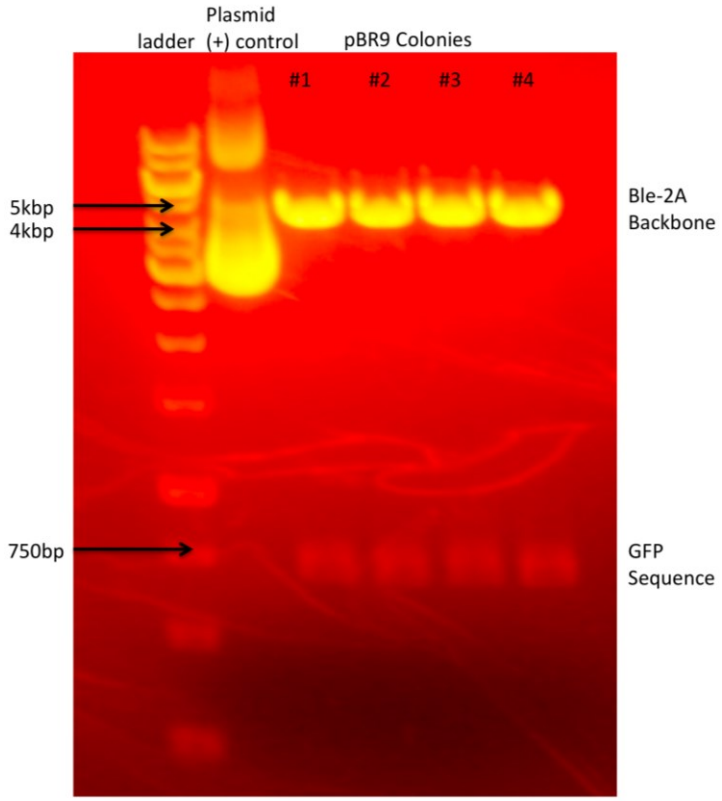

Figure 6 - Restriction enzyme digest of pBR9 for ble2A backbone

As visible in the figure above, all four pBR9 colonies had the GFP sequence excised from the plasmid. Simultaneously, the pRelax plasmid, ble-Venus-Bcl-x_L, was transformed into chemically competent *E. coli* cells and the plasmid DNA was harvested using a QIAprep Spin Miniprep kit. A Phusion PCR reaction was performed using the forward (5' to 3') primer TATCTCGAGATGGTGTCGAAGGG and the reverse (5' to 3') primer ATAAGATCTTCAGGCGCGCCTTAC. These primers surround the Venus-Bcl-x_L fusion gene with the XhoI restriction enzyme on the forward primer (underlined in the primer) to align with the pBR9 backbone's XhoI site, and a BglII restriction enzyme (underlined in the reverse primer) site to align with the BamHI site of the pBR9 plasmid.

The BglII restriction enzyme site will be able to fit with the BamHI site, but will permanently close this restriction enzyme site after ligation.

After the Phusion PCR reaction, a sample of the 1,439bp Venus-Bcl-x_L fragment was used for gel electrophoresis to confirm its amplification. The Venus-Bcl-x_L fragment from the PCR reaction was then purified using the QIAgen PCR Purification kit. After purification, the fragment was digested at 37°C for several hours with XhoI and BglII restriction enzymes to create sticky ends to fit with the pBR9 backbone. The pBR9 backbone and the Venus-Bcl-x_L insert were ligated at a 25ng : 75ng, or a 1:3, ratio using a T4 DNA Ligase for 15min at room temperature. After incubating for 15min, 4µl of the ligation was added to the thawed *E. coli* cells. The cells were placed back on ice for an additional 30min and then heat shocked at 42°C for 45sec. After the heat shock, the *E. coli* cells were placed on ice for two minutes and then given 250µl SOC media. Next, the cells were centrifuged at 3,000 rpm for 20sec. From the centrifuge, 150µl of the supernatant was removed and the *E. coli* cells were resuspended in the remaining 100µl to ensure that a high cell density would be plated. This was then plated on LB plates containing Ampicillin and allowed to grow overnight.

The colonies obtained were placed in 3ml LB media and grown overnight. The next day, a sample of the culture was held at 4°C and the rest of the culture was used for plasmid DNA extraction using a QIAprep Spin Miniprep kit. 1µg of the DNA was digested with the restriction enzyme XhoI and NcoI-HF, since the BglII/BamHI site was no longer usable. After the digest, the sample was placed in a gel and checked for two bands, one

above the 4,000bp marker, approximately 4,186bp, and another above the 1,500bp marker, approximately 1,656bp.

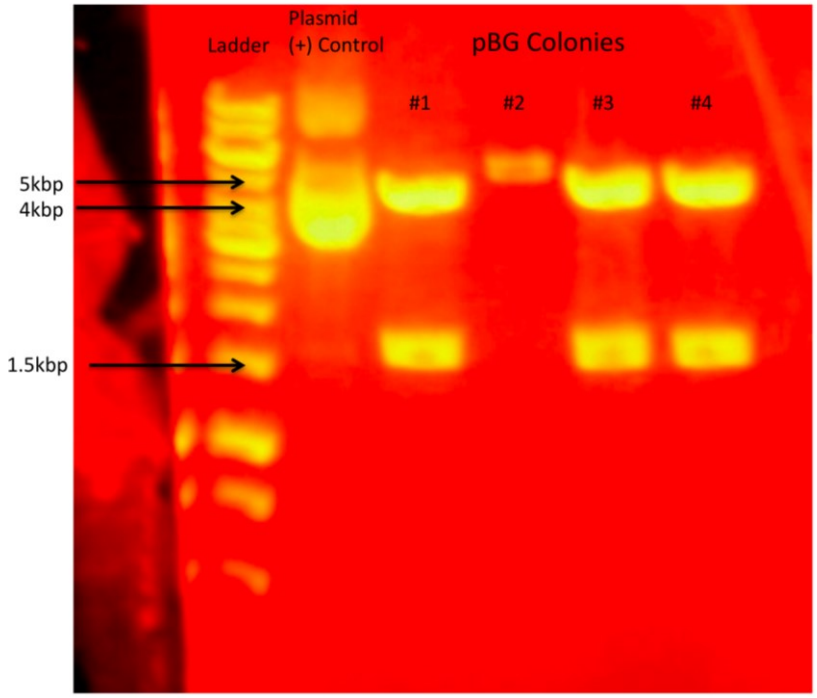

Figure 7 - Gel showing Venus-Bcl-x_L confirmation within three of the four pBG colonies

The figure above shows that three of the four colonies were successful in integrating Venus-Bcl-x_L into the ble2A backbone. With the success of the transformation, the ble2A-Venus-Bcl-x_L plasmid will now be referred to as pBG.

4.4 Nuclear transformation of *C. reinhardtii* with pBG

4.4.1 *C. reinhardtii* transformation via the Glass Bead Protocol

With the success of the pBG transformation in *E. coli*, a sample of the remaining culture was grown overnight in a 100ml flask. The next day, the plasmid DNA was harvested using a QIAgen Plasmid Midi Kit. From this plasmid stock, 1.5ug of DNA was removed and linearized using XbaI at 37°C overnight. This was replicated with a total of four samples. Two samples would be used in the *C. reinhardtii* strain UTEX 2244, and the other two samples would be used in the cell wall deficient strain, UTEX 2337.

UTEX 2244 and UTEX 2337 were grown in 50ml cultures until they reached the exponential phase. A sample was removed and resuspended in 5ml Tris-Acetate-Phosphate (TAP) Media to obtain a concentration of 50 million cells/ml. In a microcentrifuge tube, 300μl of the UTEX 2244 cell suspension was mixed with 400μg glass beads (Sigma-Aldrich, 425-600μm) and 1.5μg linearized pBG DNA. The microcentrifuge tube was vortexed at full speed for 15sec. The suspension above the glass beads was extracted and plated on a TAP plate containing 15μg/ml Zeocin (the commercially available form of the antibiotic bleomycin). After the plate dried, the plate was sealed with Parafilm and placed under constant light. This protocol was repeated for the UTEX 2337 cells. After 5-6 days, small colonies started to form.

4.4.2 *C. reinhardtii* transformation via Electroporation

An additional eight samples of 1.5µg DNA were obtained from the pBG plasmid stock. Four samples were linearized using the restriction enzyme XbaI, while the other four samples were double digested with XhoI and NcoI-HF overnight at 37°C. These restriction enzymes surround the Venus-Bcl-x_L sequence, and this process has been shown to increase transformation efficiency (Rasala et al. 2012). For a positive control, two 1.5µg samples of the original pBR9 plasmid were double digested with XhoI and BamHI-HF overnight.

UTEX 2244 and UTEX 2337 cells were grown in 50ml cultures as mentioned previously. A cell density of 400 million cells/ml was collected and placed on ice for 10min. The cells were centrifuged at 2000 x g for 5min at 4°C. The cells were resuspended in 1ml TAP media with 60mM Sucrose, and placed on ice. On ice, a 4mm electroporation cuvette (Bio-Rad Cat# 165-2081) was filled with 250µl of the cell suspension and 1.5µg linearized pBG DNA. The cuvettes were placed in a 16°C bath for 5min and then placed in the BioRad Gene Pulser II (Bio-Rad, USA) one at a time. The Gene Pulser II was set to 800kV with a capacitance of 25uF and no resistance. Each cuvette was pulsed for 5-6ms and then allowed to incubate at room temperature for 10min. The cells were then resuspended in 10ml TAP media with 60mM sucrose and allowed to incubate in low light, without shaking, for up to 24 hours.

The next day, the cells were centrifuged at 2000 x g for 5min at room temperature. The pellet was resuspended in 2ml TAP media containing 10µg/ml Zeocin for selection.

500µl of the cell suspension was plated on TAP plates containing 15µg/ml Zeocin and allowed to dry in the biosafety cabinet. Once dried, the plates were sealed in Parafilm, inverted, and placed under low light. After 5-6 days, colonies started to form.

4.5 *C. reinhardtii* transformation results

After several days, small colonies were found on the plates transformed by the glass bead protocol. In comparison, electroporation was found to outperform the glass bead method for producing colonies. All of the colonies that formed were from the UTEX 2244 species. The plates growing transformed UTEX 2337 cells did not have any colonies. Samples from the glass bead plates and samples from the electroporation plates were removed in order to test the genomic DNA for pBG integration. The samples were suspended in 50µl TE buffer, where they were placed on a heating block at 100°C for 5min. The samples were then cooled to 4°C and centrifuged at 13,000RPM for 3min. The genomic DNA in the supernatant was then extracted. Next, the Phusion PCR protocol previously mentioned was performed using 100ng of the genomic DNA from the transformed colonies and the forward and reverse primers for Venus-Bcl-x_L.

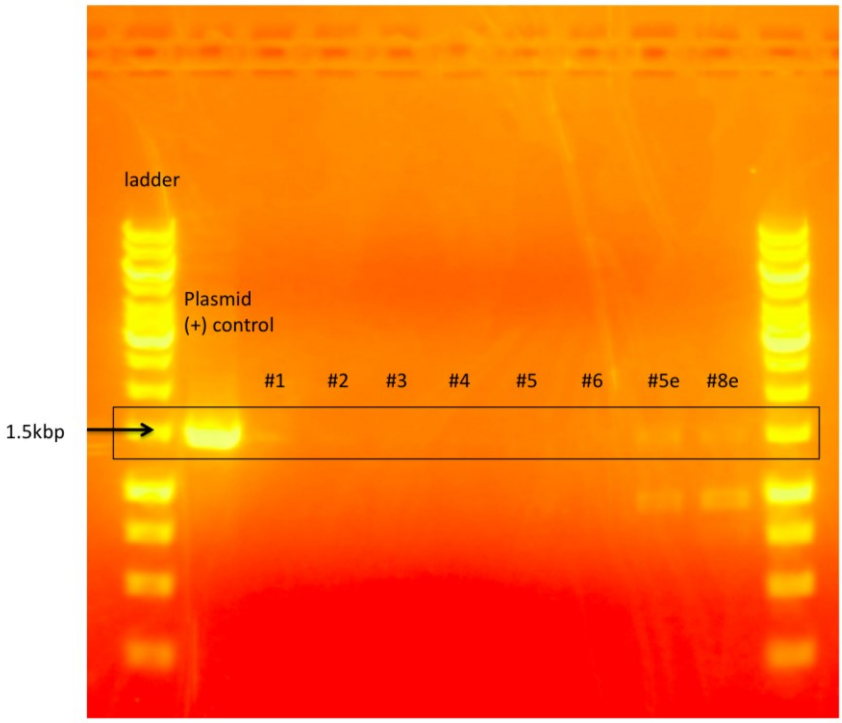

Figure 8 - Colony PCR on colonies transformed via glass bead protocol and electroporation protocol. Colonies from the electroporation protocol (5e and 8e) were found to have the Venus-Bcl-x sequence

The two colonies chosen from the electroporation plates were found to have faint bands for Venus-Bcl-x_L. With the colonies confirmed to have the Venus-Bcl-x_L sequence intact, the colonies were grown in TAP media until they reached the exponential phase and then examined for fluorescence. Several images were obtained using a Nikon Eclipse Ti Microscope.

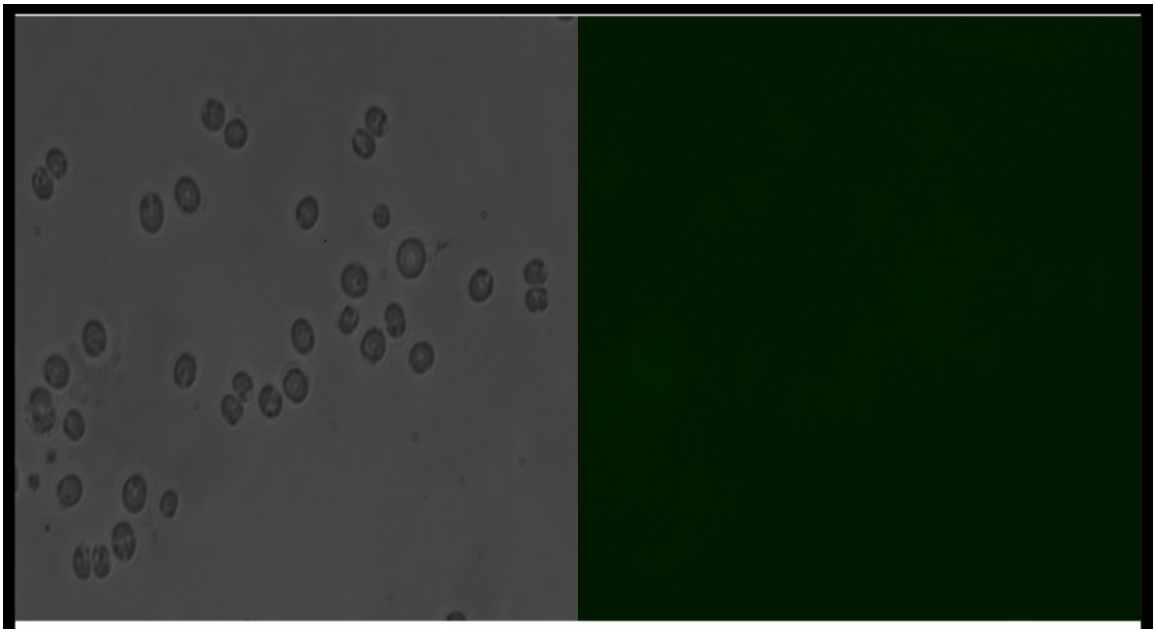

Figure 9 - Micrograph of UTEX 2244 cells at 20X magnification. The left is a phase contrast image while the right is an image taken under a FITC filter. The FITC image shows background fluorescence of the *C. reinhardtii* cells, indicating no Venus protein.

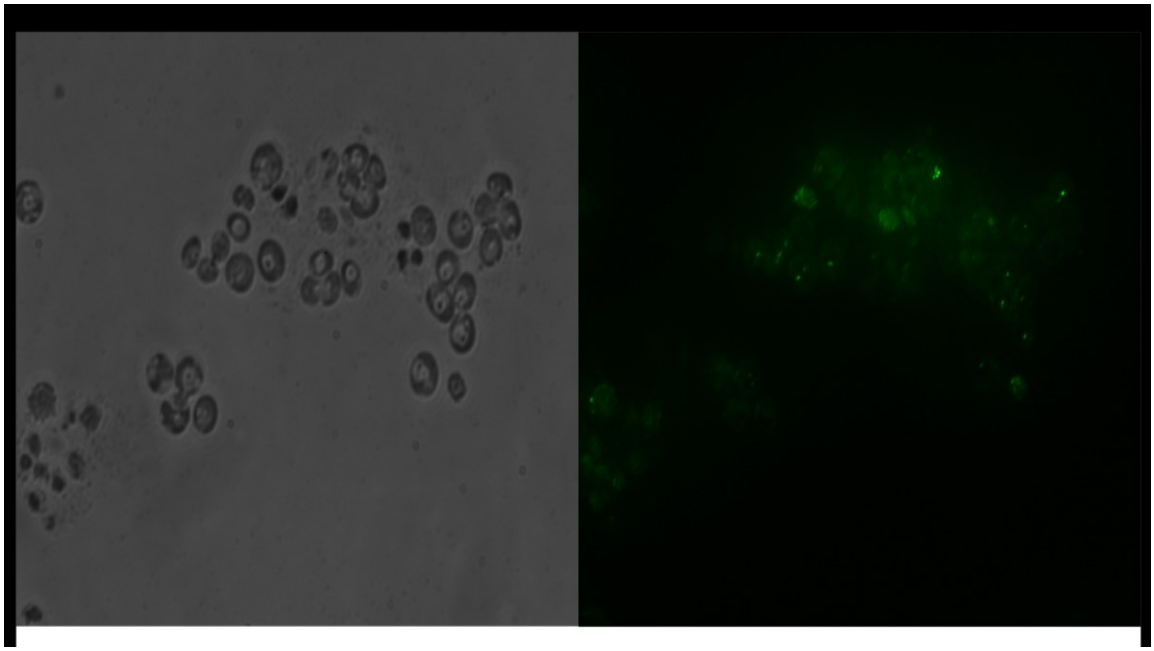

Figure 10 - Micrograph of colony #5 of the pBG cell line at 20X magnification. The left is a phase contrast image while the right is a fluorescent image using a FITC filter. Pockets of fluorescence are visible amongst the background fluorescence of the *C. reinhardtii* cells.

4.6 Transformation Conclusion

From the gel images, the incorporation of the Venus-Bcl-x_L sequence into the ble2A backbone proved successful. This was properly transformed into the *C. reinhardtii* cell line UTEX 2244 via electroporation as the genomic DNA was found to contain the Venus-Bcl-x_L sequence. Lastly, in order to check for protein synthesis, fluorescent images were taken compared to the negative control of UTEX 2244. From the micrographs, the pBG *C. reinhardtii* cells contain pockets of fluorescence, showing what can be inferred as Venus-Bcl-x_L protein production on the membrane of the mitochondria.

During the transformation process to insert the pBG plasmid into *C. reinhardtii*, the plasmid was unable to insert itself into the UTEX 2337, or the cell wall deficient strain, cells. One week after electroporation, no colonies had formed on the plates labeled "pBG-2337". One method to improve upon electroporation for cells without a cell wall has been documented by Rasala et al. This would include increasing the resistance of the BioRad Gene Pulser II to 200, from zero, and adding in 100μg/ml arginine to the media, which helps in cell recovery [72]. Making this modification in the protocol would enhance the transformation process and cell recovery.

The fluorescent micrographs are another point of interest. These images were obtained using a Nikon Eclipse Ti Microscope with the FITC filter. FITC, or fluorescein isothiocyanate, is known to have a peak excitation and emission spectrum at 495nm and

519nm, respectively. The Venus fluorescent protein has an excitation peak at 514nm and 527nm. Therefore, under the FITC filter, the Venus fluorescent protein will be excited and visible. The problem lies in the excitation of chlorophyll within the cell. Chlorophyll has the capability of fluorescing within this range. This is one of the reasons why a dim fluorescence is visible in the UTEX 2244 cell images. To ensure the fluorescence in pBG is correctly attributed to Venus-Bcl-x_L, a western blot can be performed to show protein expression, as well as confocal imaging to narrow the wavelength and reduce background fluorescence.

Chapter 5: Environmental Stress Adaptability of *C. reinhardtii*

5.1 Salt Tolerance and Influence

As mentioned previously, Sodium Chloride (NaCl) can stress algae cells in three ways: ionic, osmotic, and oxidative stress. This stress on the cells can cause initial damage through swelling and rupturing, as well as an imbalance in salt homeostasis. Previous work in lab has shown that 150mM NaCl begins to induce apoptosis in *C. reinhardtii*, as well as concentrations as high as 250mM can begin to induce necrosis [78]. The salt adaptability study was explored in the pBG cell line containing the anti-apoptotic gene Bcl-x_L. To prove that pBG is more tolerant and able to resist apoptosis, a negative control, UTEX 2244, was placed under the same stress. Additionally, pBR9 (ble2A-GFP), the plasmid that pBG was derived from, was used as an additional control. The addition of pBR9 to the salt adaptability study would demonstrate that the Venus-Bcl-x_L sequence allows for a greater salt tolerance than the pBR9 cell line, which does not contain an anti-apoptotic gene sequence.

5.2 *C. reinhardtii* Exposure to Salt

The *C. reinhardtii* cell lines UTEX 2244 (wild type), pBR9, and pBG were used for the salt stress experiment. Each cell line was broken into three groups, a control group receiving no salt, a group receiving 150mM Sodium Chloride (NaCl), and a group receiving 250mM NaCl. A 4M NaCl stock solution was prepared for the study. The cell lines were inoculated in 10ml of TAP media in a 25ml Tissue Culture Flask at a starting

concentration of 200,000 cells/ml. The cultures were placed on an Innova 2100 Platform Shaker at 60 RPM with constant motion and continuous light. Every 12 hours, samples from the cultures would be removed and inserted in the Guava Personal Cell Analysis (PCA) System ("Guava") to determine cell density and cell viability. As the cell lines reached approximately 1,000,000 cells/ml, they were stressed with either TAP media (for the control groups), 150mM Sodium Chloride (NaCl), or 250mM NaCl. The control groups received TAP media equal to the 250mM NaCl volume, while the groups that received 150mM NaCl also received TAP media to reach the same volume. The cultures were then placed back on the orbital shaker for an additional hour before the cell density was measured via the Guava. After the addition of NaCl, samples were taken every 12 hours to monitor the cultures' ability to adapt to the altered conditions.

5.3 Oxidative Stress Tolerance and Influence via Rose Bengal

Rose Bengal is a photosensitizing dye that can induce photooxidative stress in algae. Its reaction involves the formation of a singlet oxygen ($^1O_2$) from an excited photosensitizer in the chloroplast [79]. The addition of Rose Bengal to an algae cell can lead the cell directly to apoptosis. Previous lab research shows that Rose Bengal is able to induce apoptosis in *C. reinhardtii* in the micromolar range. With this knowledge, UTEX 2244, pBR9 and pBG cell lines will be stressed with 2μM and 10μM concentrations of Rose Bengal to see how the cell lines will adapt to the photooxidative stress.

5.4 *C. reinhardtii* Exposure to Rose Bengal

Similar to the Salt stress study, each cell line was broken into three groups, a control group receiving no stress, a group receiving 2μM Rose Bengal (RB), and a group receiving 10μM RB. A 1mM RB stock solution was prepared for the study. The cell lines were inoculated in 10ml of TAP media at a starting concentration of 200,000 cells/ml. The cultures were placed on an Innova 2100 Platform Shaker at 60 RPM with constant motion and continuous light. Every 12 hours, samples were taken and analyzed by the Guava to determine cell density and cell viability. As the cell lines reached approximately 1,000,000 cells/ml, they were stressed with either TAP media (for the control groups), 2μM RB, or 10μM RB. The control groups received TAP media equal to the 10μM RB volume, while the groups that received 2μM RB also received TAP media to reach the same volume. The cultures were then placed back on the orbital shaker for an additional hour before the cell density was measured. After the addition of RB, samples were taken every 12 hours to monitor the cultures' ability to adapt to the stress.

5.5 Cell Density and Cell Viability via Guava

The Guava Personal Cell Analysis (PCA) System ("Guava"; Millipore) is a flow cytometer that, coupled with the Guava ViaCount Software, is able to differentiate between living and dead cells. Each cell passes through the system and is detected, determining whether the cell is alive or induced apoptosis or necrosis. After the sample is measured, the Guava produces the calculated cell density (cells/ml) based on dilution factor and total volume of the culture. Along with the cell density is the cell viability,

which determines what percent of the sample contains viable cells, apoptotic cells, and necrotic cells.

5.6 Cell Adaptability Results

The salt and Rose Bengal studies were conducted over the course of 78 hours. Each cell line grew at different rates, so the stresses were administered when the cell line's cultures reached 1,000,000 cells/ml. This occurred around 30 hours for pBG, 54 hours for UTEX 2244, and 66 hours for pBR9.

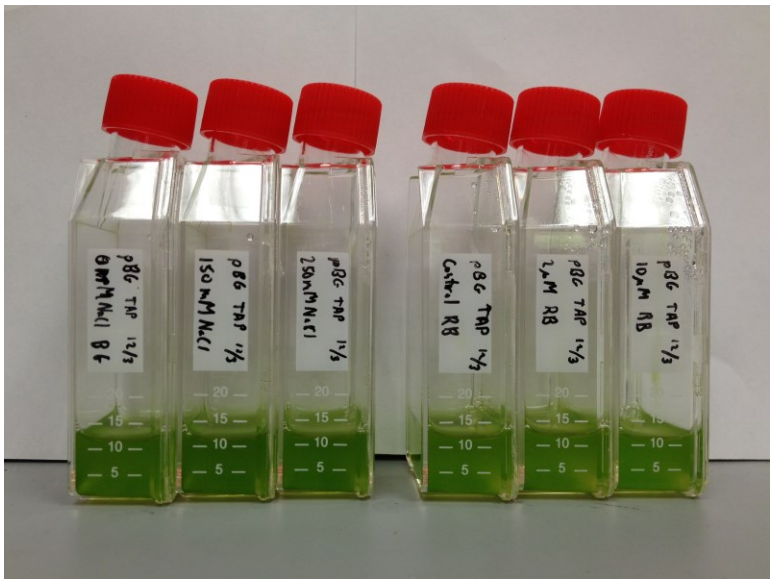

Figure 11 - 10ml pBG cultures at approximately one million cells/ml before NaCl and RB were applied.

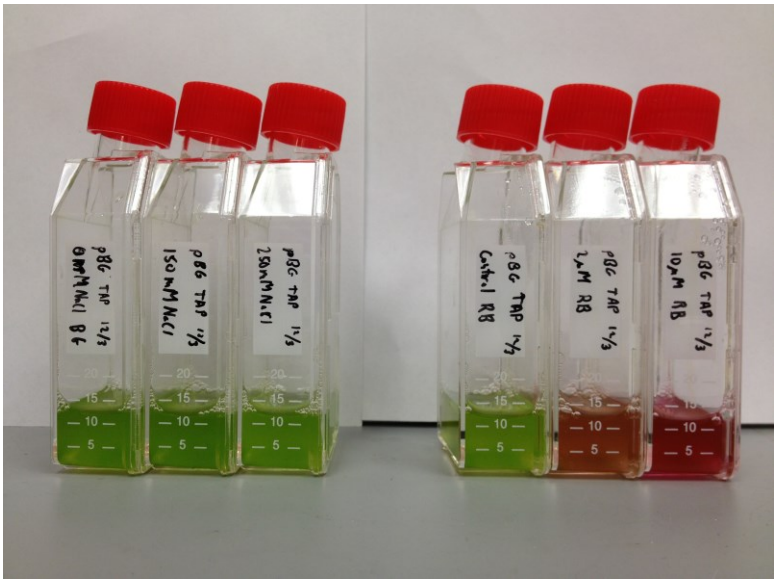

Figure 12 - 10ml pBG cultures immediately after NaCl and RB were added. NaCl cultures are on the left, and RB cultures are on the right.

At one million cells/ml, the cultures had already entered the exponential phase of growth. During this time period, pBG cultures are expected to contain Bcl-x_L. The addition of NaCl and RB to the pBG cultures will induce oxidative stress and is expected to lead to an increase in Bcl-x_L production. From the figures above, it is difficult to see any reaction to the addition of NaCl, but the addition of RB stains the cells red, leading to the colors seen above. Additionally, the 10µM RB culture is a darker red than the culture that received 2µM. This demonstrates that the smaller concentration of RB will allow the pBG line to adapt quicker and maintain higher cell density and cell viability.

5.6.1 Salt Stress Analysis

The three cell lines were exposed to 0mM, 150mM, or 250mM NaCl. Their cell density and cell viability were recorded approximately every 12 hours, including an additional

measurement one hour after salt exposure. The light blue background on the graphs represents the time period in which NaCl was present in the culture.

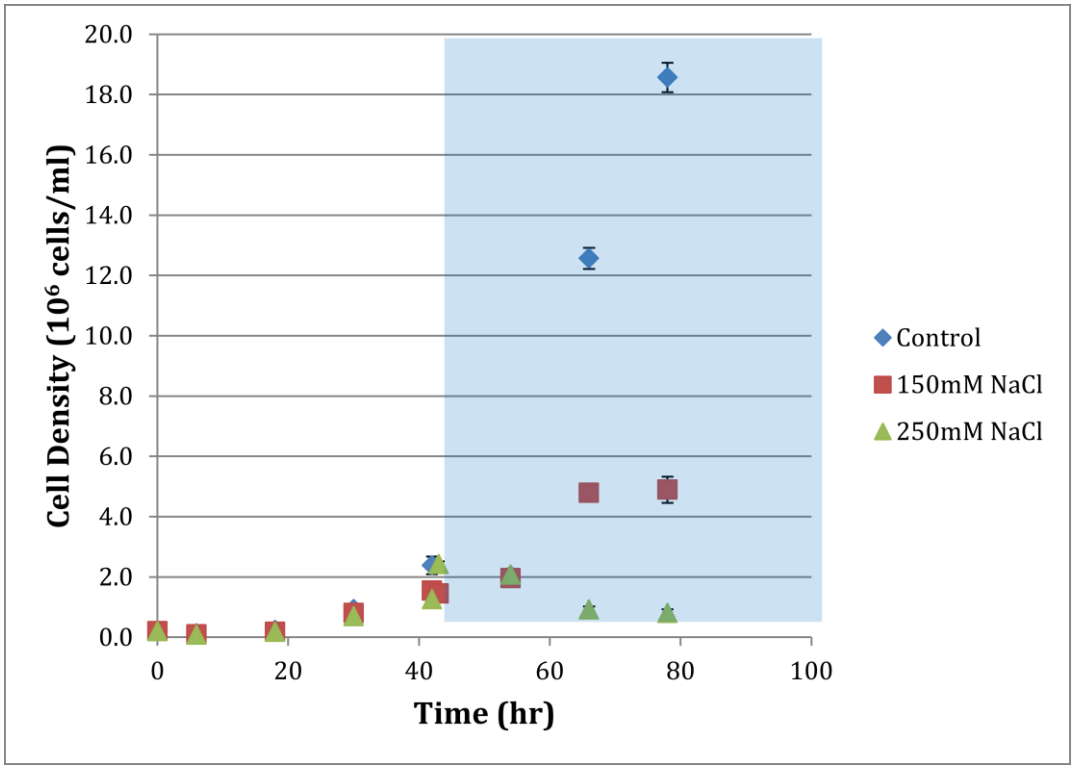

Figure 13 - NaCl stress adaptability curve of UTEX 2244 (wildtype). Stress added 42 hours after inoculation.

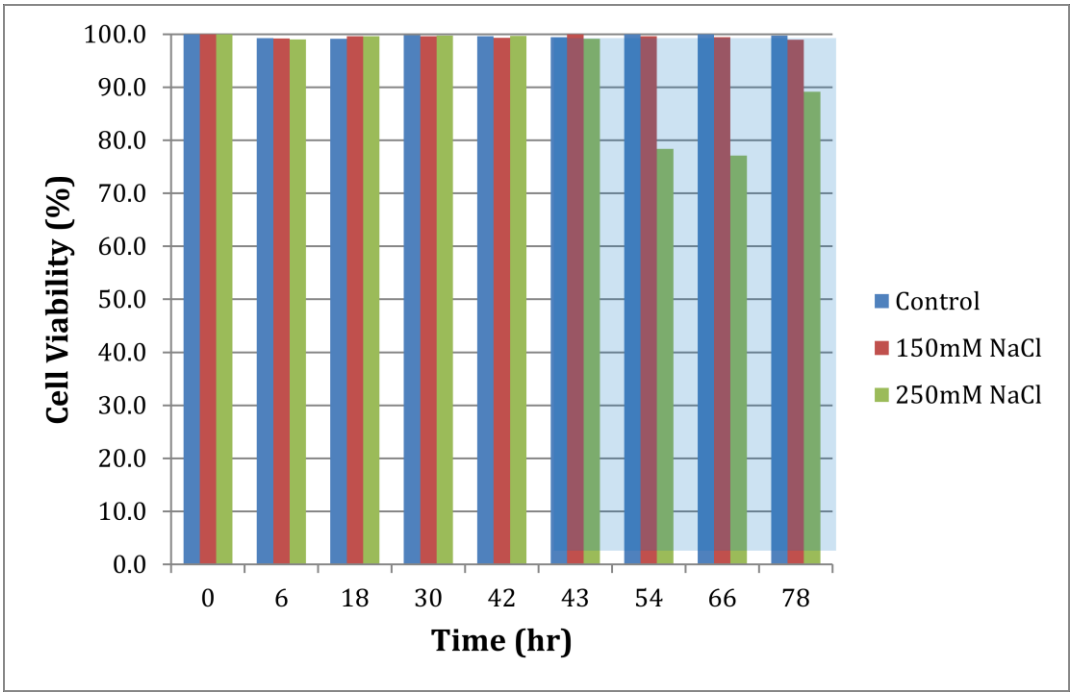

Figure 14 – UTEX 2244 cell viability before and after NaCl stress.

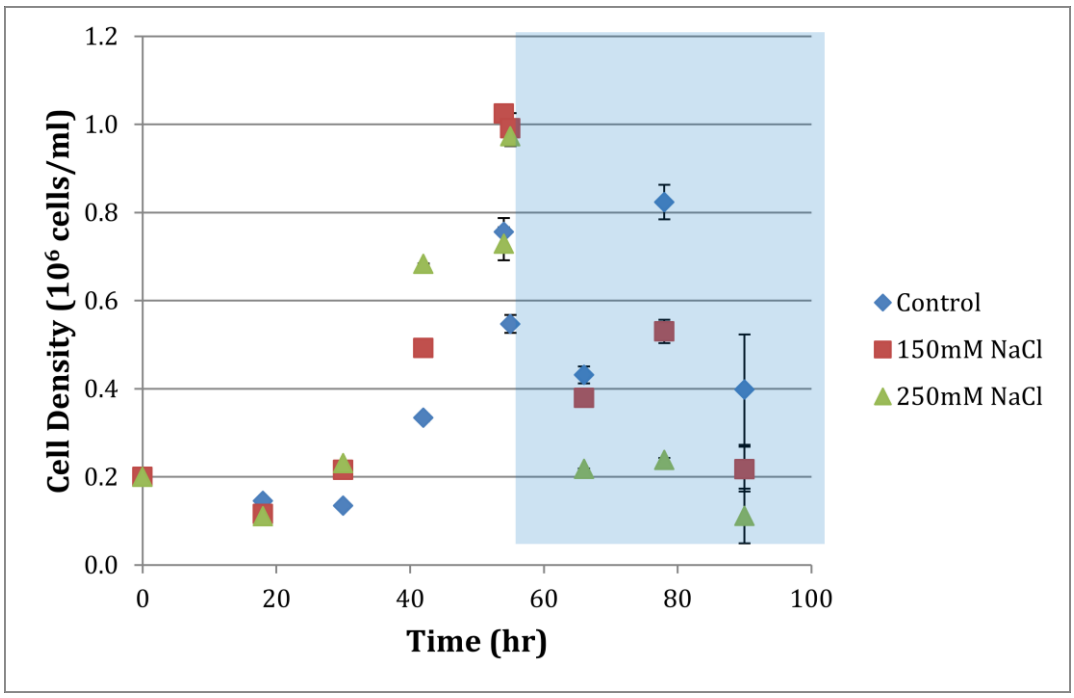

Figure 15 -NaCl stress adaptability curve of pBR9 (negative control). Stress added 54 hours after inoculation.

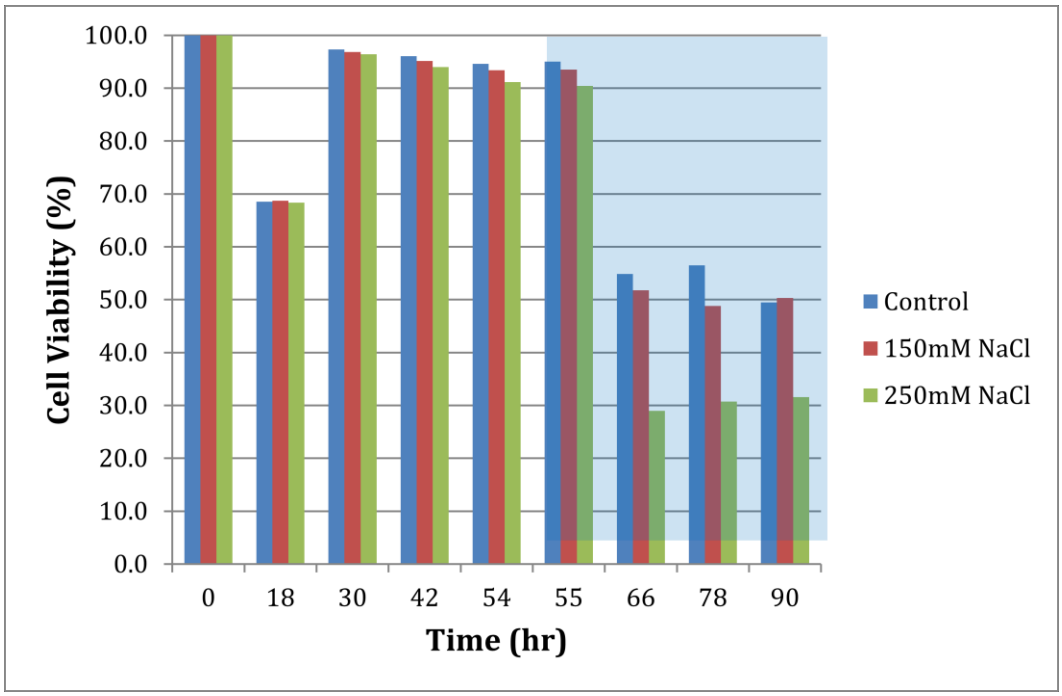

Figure 16 – pBR9 cell viability before and after NaCl stress.

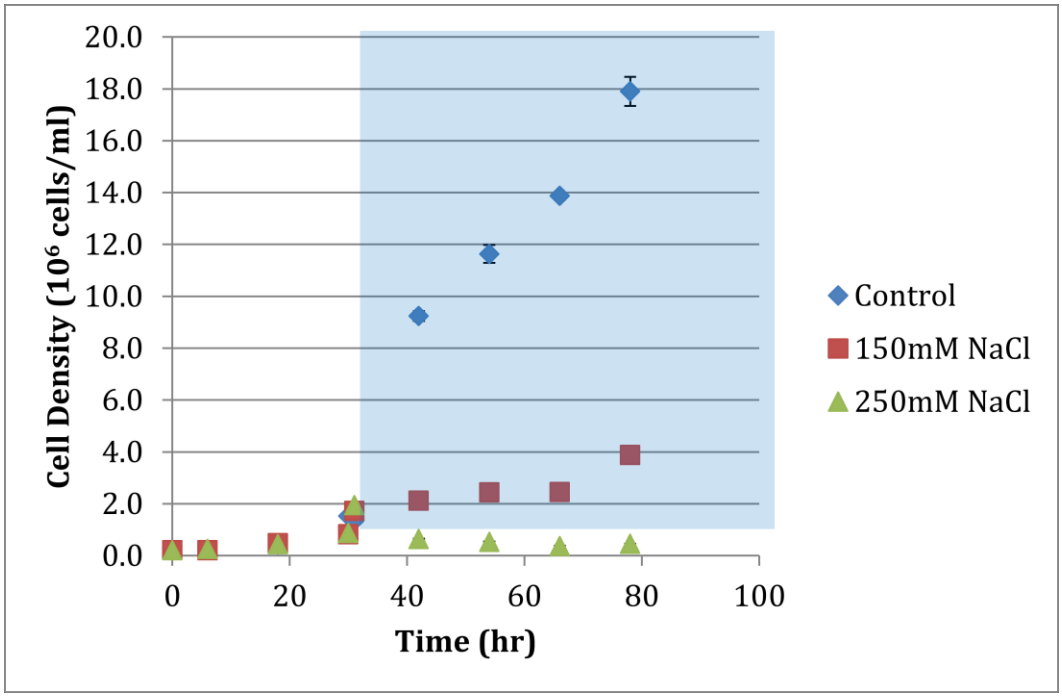

Figure 17 - NaCl stress adaptability curve of pBG. Stress added 30 hours after inoculation.

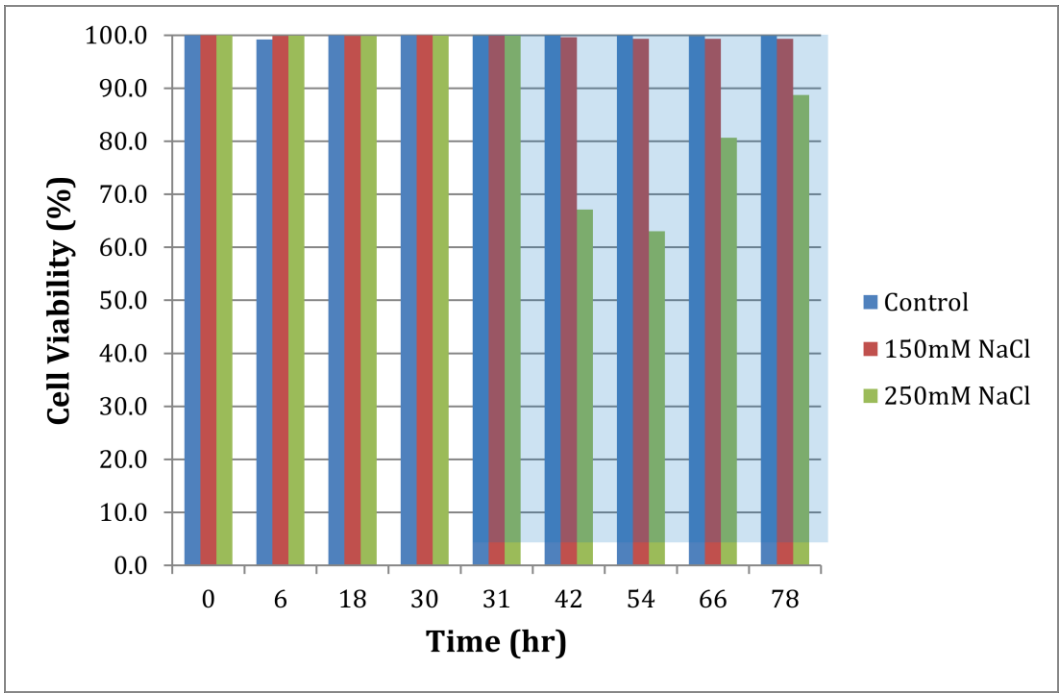

Figure 18 - pBG cell viability before and after NaCl stress.

The addition of NaCl at 150mM and 250mM concentrations begins to induce cell death as cell viability decreases 12 hours after stress. The cultures were in the exponential growth phase when the stress was added. Once stressed, the cells are forced to adjust to the high salt concentration. This is seen by the reduction of growth of UTEX 2244 and pBG 12 to 24 hours after stress. The 250mM NaCl stress reduced cell viability by 22% and 33% of UTEX 2244 (with 1.26 million viable cells/ml) and pBG (with 0.867 million viable cells/ml), respectively. While this initial data shows that the wildtype, UTEX 2244, had 11% greater viability 12 hours after stress, both cultures were able to recover to 89% viability with less than 1 million cells/ml.

While the UTEX 2244 and pBG cultures maintained high cell viability and consistent growth rate, the pBR9 cell line experienced a slightly lower cell viability percentage and a slower growth rate. The pBR9 cell line was not stressed until the 54-hour time point. This is 12 hours after stressing UTEX 2244 and 24 hours after pBG. Moreover, the addition of NaCl decreased cell viability to less than 50%. However, this cannot be confirmed as to NaCl stress, as the viability of the control also decreased to approximately 50% when only TAP media was added. Therefore, the study remains inconclusive, as the pBR9 culture did not maintain high cell viability for the control.

5.6.2 Rose Bengal Stress Analysis

The three cell lines were exposed to 0μM, 2μM, or 10μM Rose Bengal (RB). Their cell density and cell viability were recorded approximately every 12 hours, including an additional measurement one hour after salt exposure. The light red background on the graphs represents the time period in which RB was present in the culture.

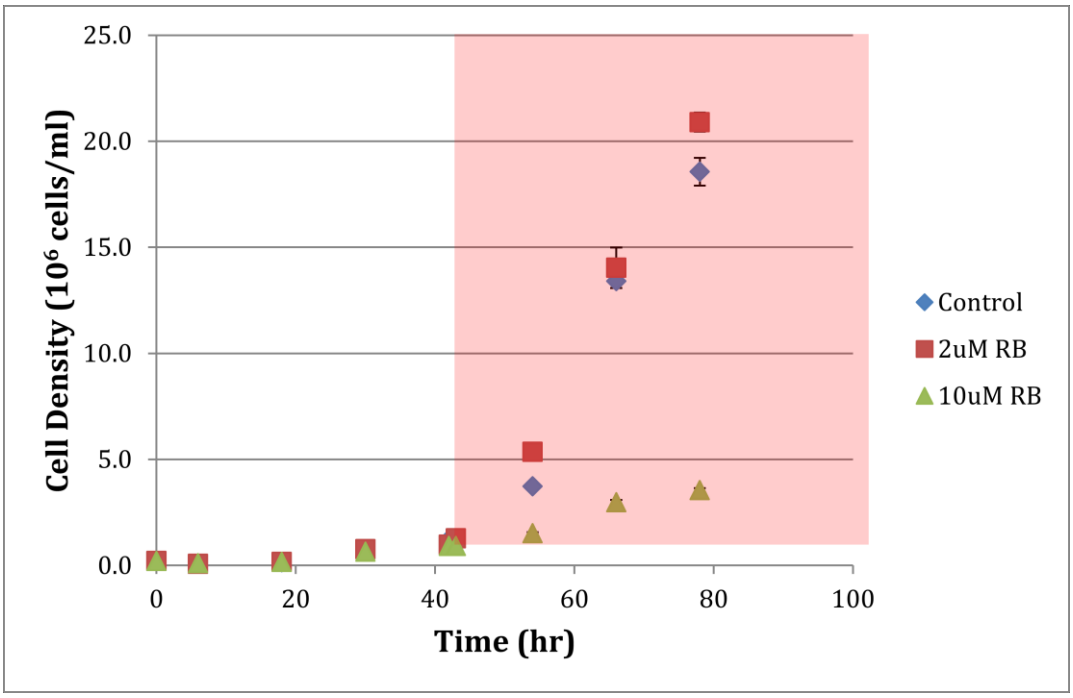

Figure 19 – RB stress adaptability curve of UTEX 2244 (wildtype). Stress added 42 hours after inoculation.

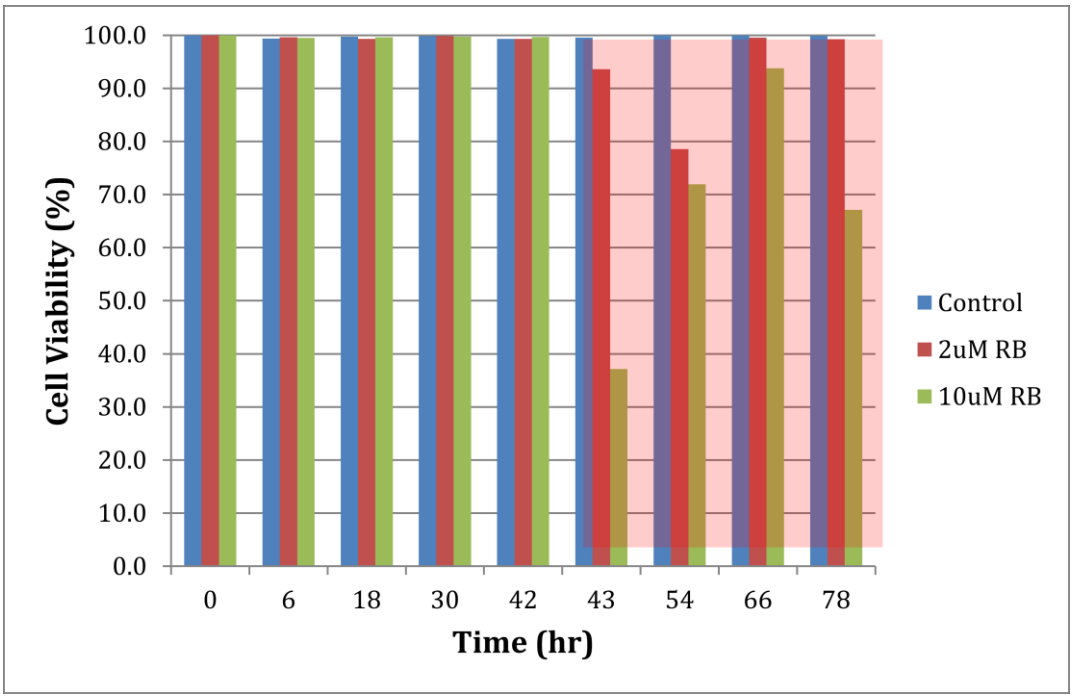

Figure 20 – UTEX 2244 cell viability before and after RB stress.

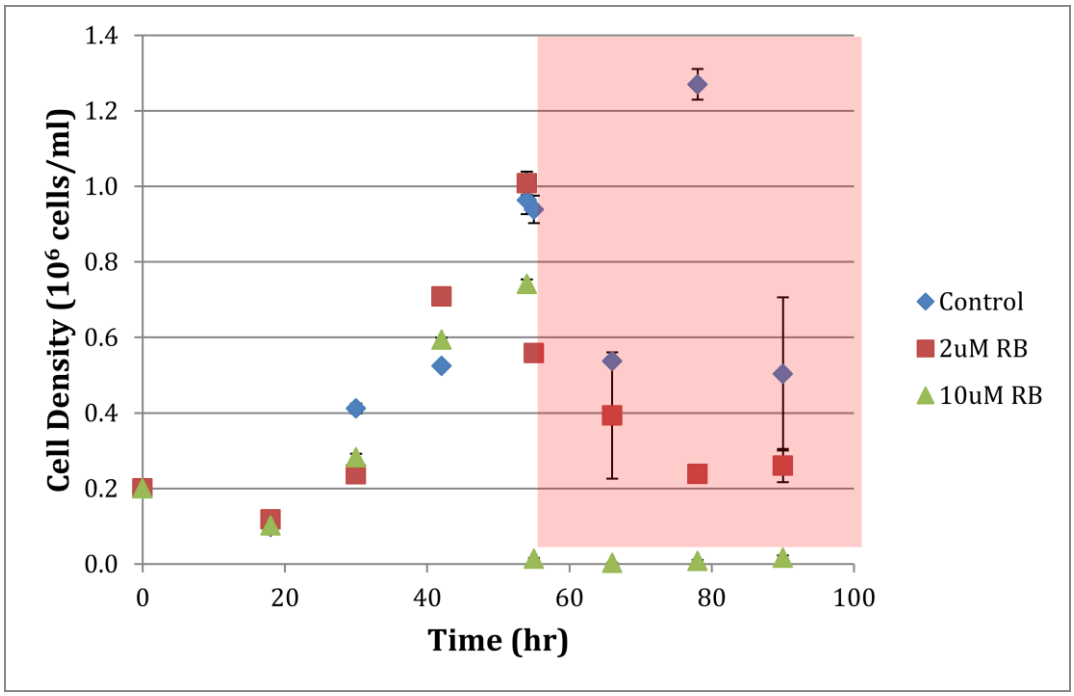

Figure 21 – RB stress adaptability curve of pBR9 (negative control). Stress added 54 hours after inoculation.

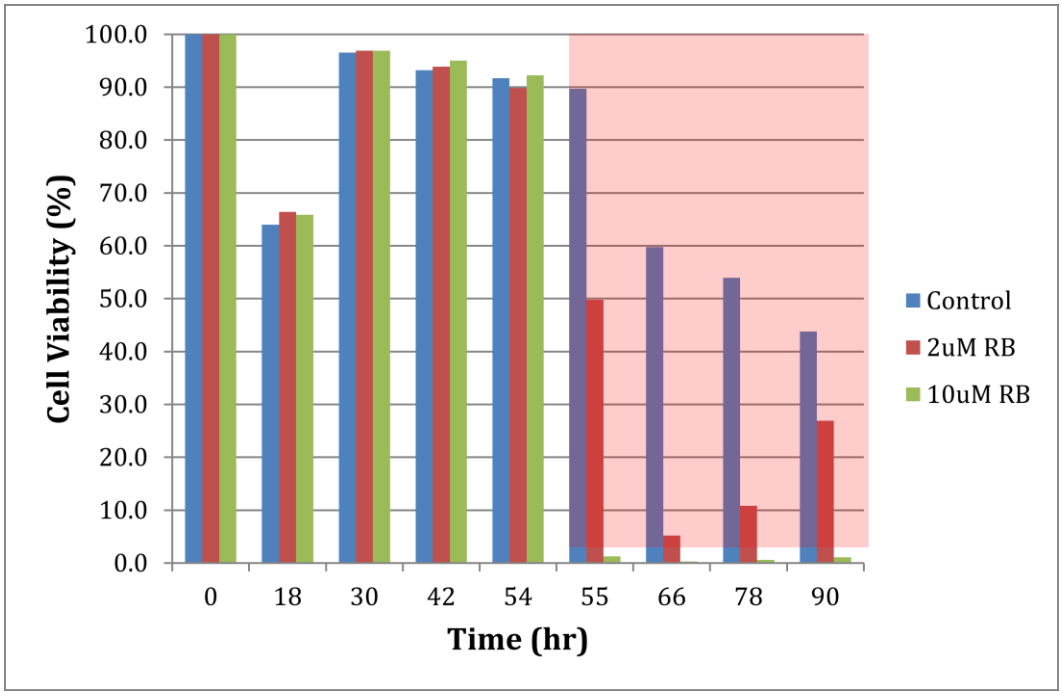

Figure 22 - pBR9 cell viability before and after RB stress.

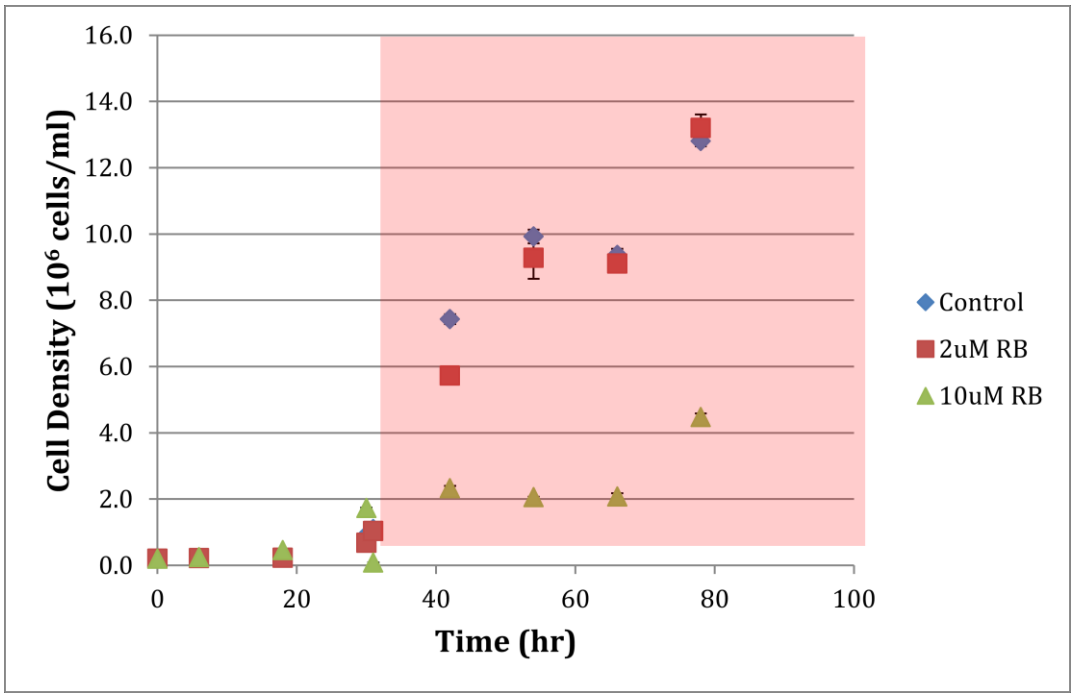

Figure 23 – RB stress adaptability curve of pBG. Stress added 30 hours after inoculation.

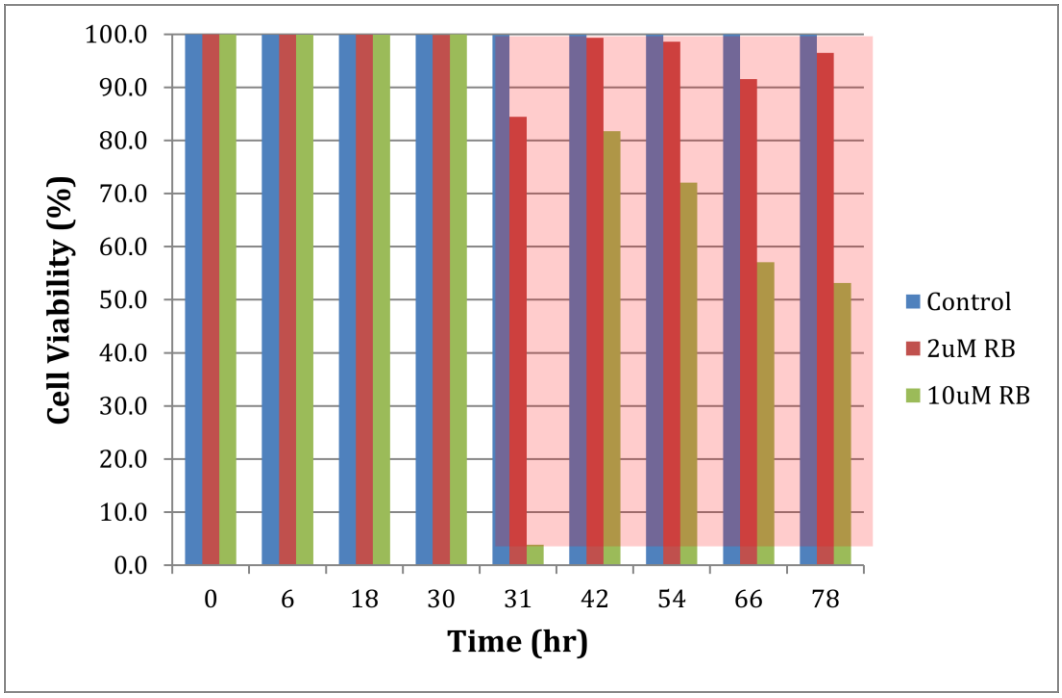

Figure 24 – pBG cell viability before and after RB stress.

The addition of Rose Bengal (RB) in 2μM and 10μM concentrations induced photooxidative stress on the cells, leading to apoptosis and cell death. It was found that the 2μM RB concentration was not enough to lower cell viability below 75% percent in the UTEX 2244 and pBG cell lines, but was able to lower the cell viability to 50% in pBR9. After the 2μM RB stress, the UTEX2244 and pBG cell lines were able to recover and maintain at least 90% cell viability. The addition of 10μM RB was able to halt cell growth and force cell repair in all of the cell lines. Twelve hours after RB stress, UTEX 2244 maintained 72% cell viability (with 1.52 million viable cells/ml), while pBG maintained 82% cell viability (with 2.33 million viable cells/ml). Even though this shows that pBG maintains higher cell viability 12 hours after stress, the data shows cell viability decreasing to approximately 50% for pBG as the cell density increases, while the cell viability for UTEX 2244 fluctuates between 60% and 90%.

In pBR9, the addition of 10μM RB reduced viability to less than one percent for the remainder of the study. Similar to the NaCl stress study, the addition of the TAP media for the control reduced cell viability to approximately 50%. This once again shows that the pBR9 data remains inconclusive, as the media addition should not induce cell death. This could potentially be due to bacterial infection of the culture. The best measure to properly replicate the study would be to filter all media components and closely monitor the culture for infection.

5.7 Confocal Imaging

The confocal images were obtained at the Integrated Imaging Center (IIC) using a LSM 510 Zeiss microscope with the Zen Software. The three cell lines imaged were UTEX 2244, pBR9-Venus, and pBG. The UTEX 2244 and pBR9-Venus samples were obtained from previously growing cell cultures. The pBG sample was obtained from the 10μM RB culture. The reason for choosing the pBG sample from this culture was because of the cell culture's survivability. Eighteen hours after the addition of Rose Bengal, the culture maintained 82% cell viability. The cells that survived photooxidative stress would most likely contain Venus-Bcl-x_L within the cell. The cells that silenced transcription of the Venus-Bcl-x_L gene would have a better chance of degradation and becoming debris. The UTEX 2244 cells are wildtype and therefore would not fluoresce, while the pBR9-Venus cells are a positive control to show YFP fluorescence. These Brightfield micrographs are imaged at 20X magnification and with a FITC filter overlap.

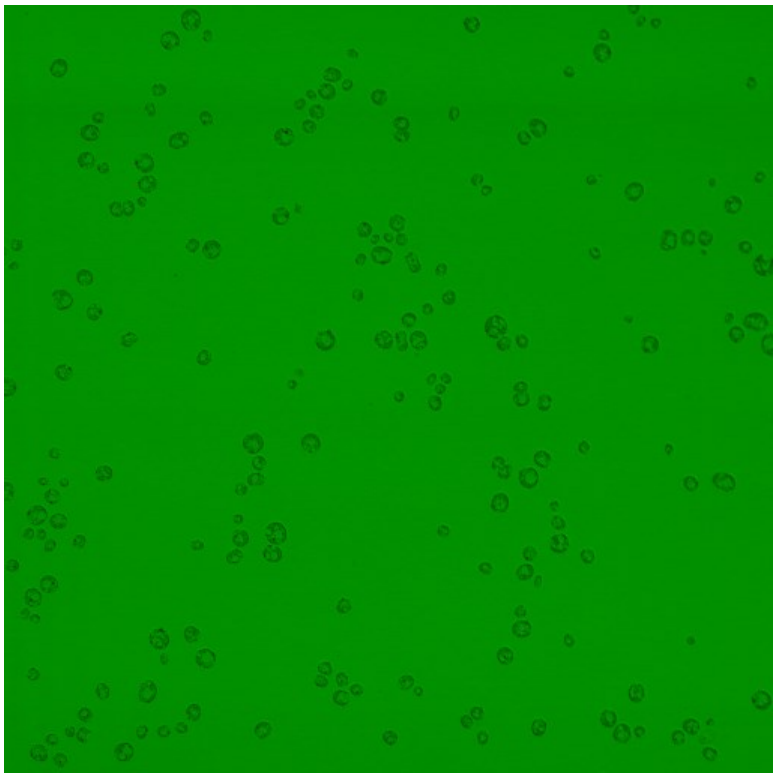

Figure 25 - UTEX 2244 confocal micrograph. Cells were not stressed before imaging. Image shows no fluorescence on the wild type cells.

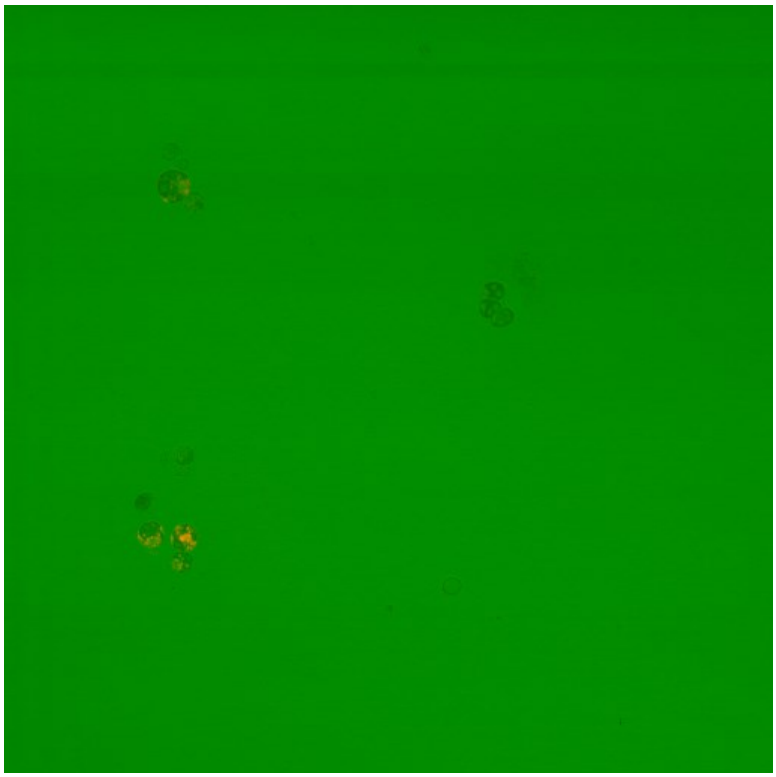

Figure 26 - pBR9 confocal micrograph. Cells were not stressed before imaging. Image shows fluorescence throughout the cell.

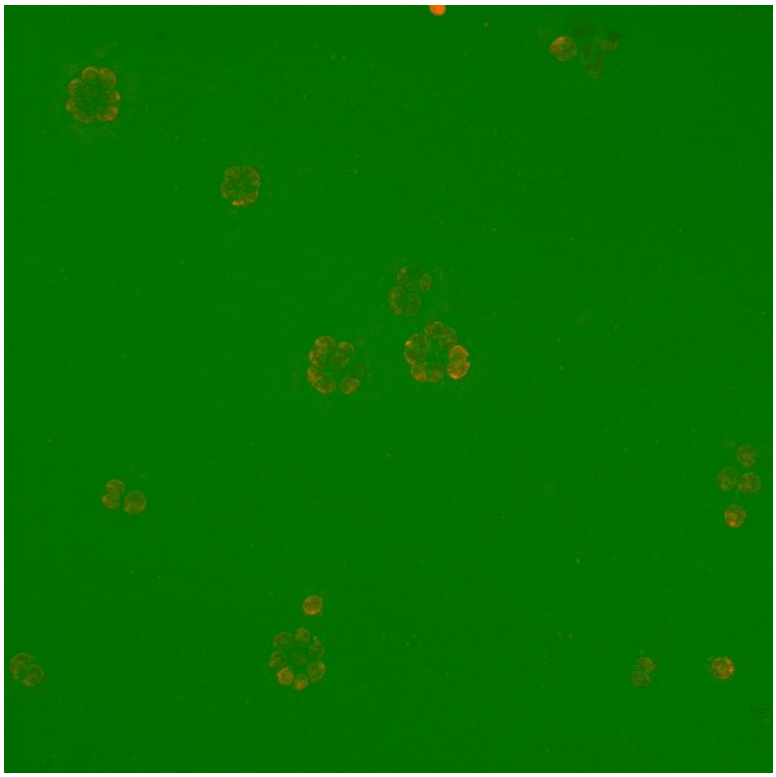

Figure 27 – pBG confocal micrograph. Cells were stressed with 10µM Rose Bengal 18 hours before imaging. Image shows fluorescence throughout multiple cells. Cells maintained approximately 82% viability after previous time point.

The confocal images were specifically taken to reduce background fluorescence of the cell. This includes narrowing the emission/excitation spectrum so that the confocal microscope would be able to excite Venus at approximately 514nm. The images confirm UTEX 2244 without fluorescence while pBR9-Venus cells contain fluorescence throughout some of the cells at the bottom left of the micrograph. At the top left of the pBR9-Venus micrograph, fluorescence is still visible but in smaller amounts. As for the pBG micrograph, the cells were grouped together. These cells do not have localized fluorescence as the micrographs in Chapter 4 display.

5.9 Discussion

Salt and photooxidative stress are known to induce programmed cell death (PCD) when delivered at the concentrations tested. The viability of UTEX 2244, pBR9, and pBG were found to have decrease after the stress, and in the case of UTEX 2244 and pBG the cultures were able to recover. This shows that pBG has similar adaptability as the wildtype, and Bcl-x_L was only able to show a decrease in cell death when stressed with Rose Bengal. On the other hand, pBR9, the source of the pBG plasmid, was not able to recover from the stresses. Though, this study needs to be performed again on pBR9 to confirm that Bcl-x_L in pBG allows for an increase in cell viability.

In order to confirm that Bcl-x_L protein production, confocal images were taken of pBG cells after inducing photooxidative stress. The micrographs show comparable fluorescence to the pBR9-Venus cells, and in more cells. This confirms the production of the Venus within the cell, and it is possible to infer that the Bcl-x_L protein is being expressed as well. This can be confirmed with a western blot. A western blot was performed with the pBG samples, using the pBR9-Venus protein as a positive control for Venus expression. The resulting membrane displayed no protein expression. This may be due in part that the cultures maintained low cell density and did not have enough protein expressed. It is also possible that the protein extraction protocol was not optimized for mitochondrial protein, and the extraction will need to be adjusted.

6. Future Goals

With the completion of the stress adaptability study and confocal micrographs confirming fluorescence, the pBG cell line contains a strong transgene expression. A replication of the stress adaptability study for the pBR9 cell line would aid in confirming that the addition of the Bcl-x_L protein in pBG improves cell viability and decreases cell death. The next goal is to perform a western blot on the pBG cell line with a high cell density. This will be done in comparison with UTEX 2244 (the negative control) and pBR9-Venus (positive control) for Venus expression.

With an increase in transgene expression, the next goal would be to compare the use of the Foot and Mouth Disease Virus (FMDV) 2A peptide sequence against Matrix Attachment Regions (MARs). Previous studies have shown that surrounding the transgene with two MAR sequences will allow for increased expression. The study will be measuring expression levels, whether it is a fluorescent protein or Venus-Bcl-x_L, of MARs within *C. reinhardtii*. MARs have not been implemented in *C. reinhardtii*, so the study will analyze expression levels of: Gene of Interest (GOI) as a standard, ble2A-GoI, MARs before the GoI, MARs after the GoI, and MARs before and after the GoI. After determining which sequence produces the greatest expression, it will be interesting to see if the addition of MARs before and after the ble2A-GoI improves overall expression levels.

References

[1] United States Environmental Protection Agency. "EPA Finalizes 2013 Renewable Fuel Standards." Office of Transportation and Air Quality. August 2013. http://www.epa.gov/otaq/fuels/renewablefuels/documents/420f13042.pdf

[2] United States Environmental Protection Agency. "EPA Proposes 2014 Renewable Fuel Standards, 2015 Biomass-Based Diesel Volume." Office of Transportation and Air Quality. November 2013. http://www.epa.gov/otaq/fuels/renewablefuels/documents/420f13048.pdf

[3] Sapphire Energy. "Statement from Vice President of Corporate Affairs Tim Zenk, Regarding EPA Announcement of Renewable Fuel Targets." November 15, 2013. http://www.sapphireenergy.com/documents/SE%20RVO%20Statement%2011-15-13.pdf

[4] Wan, Minxi, et al. "The effect of mixotrophy on microalgal growth, lipid content, and expression levels of three pathway genes in *Chlorella sorokiniana*." *Applied microbiology and biotechnology*, 2011, 91.3, 835-844.

[5] Q. Hu, M.S. *Photobioreactor: System and Process*. *Algae Biomass Summit*. 2008.

[6] Chiu, Sheng-Yi, et al. "Lipid accumulation and CO2 utilization of *Nanochloropsis oculata* in response to CO2 aeration." *Bioresource Technology*, 2009, 100.2, 833-838.

[7] Zhu, JK. "Salt and drought stress signal transduction in plants." *Annual Review of Plant Biology*, 2002, 53, 247–273.

[8] Affenzeller, Matthias Josef, et al. "Salt stress-induced cell death in the unicellular green alga *Micrasterias denticulata*." *Journal of Experimental Botany*. 2009, Vol. 60, No. 3, 939-954.

[9] Zhu, JK. "Salt Plant Tolerance." *Trends in Plant Science*, Volume 6, Issue 2, 1 February 2001, Pages 66–71.

[10] Bérubé KA, Dodge JD, Ford TW. "Effects of chronic salt stress on the ultrastructure of *Dunaliella bioculata* (Chlorophyta, Volvocales): mechanisms of response and recovery." *European Journal of Phycology,* 1999, 34, 117–123.

[11] Takagi M, and Karseno Yoshida T. “Effect of salt concentration on intracellular accumulation of lipids and triacylglyceride in marine microalgae *Dunaliella* cells.” *Journal of Bioscience and Bioengineering,* 2006, 101, 223–226.

[12] Goyal A. “Osmoregulation in *Dunaliella*. II. Photosynthesis and starch contribute carbon for glycerol synthesis during a salt stress in *Dunaliella tertiolecta*.” *Plant Physiology and Biochemistry,* 2007, 45, 705–710.

[13] Yoshida K, Igarashi E, Wakatsuki E, Miyamoto K, Hirata K. “Mitigation of osmotic and salt stresses by abscisic acid through reduction of stress-derived oxidative damage in *Chlamydomonas reinhardtii*.” *Plant Science,* 2004, 167, 1335–1341.

[14] Orosa M, Valero JF, Herrero C, Abalde J. “Comparison of the accumulation of astaxanthin in *Haematococcus pluvialis* and other green microalgae under N-starvation and high light conditions.” *Biotechnology Letters,* 2001, 23, 1079–1085.

[15] Pelah D, Sintov A, Cohen E. “The effect of salt stress on the production of canthaxanthin and astaxanthin by *Chlorella zofingiensis* grown under limited light intensity.” *World Journal of Microbiology and Biotechnology,* 2004, 20, 483–486.

[16] Boussiba S, and Vonshak A. “Astaxanthin accumulation in the green alga *Haematococcus pluvialis*.” *Plant and Cell Physiology*, 1991, 32, 1077–1082.

[17] Boussiba S. “Carotenogenesis in the green alga *Haematococcus pluvialis:* Cellular physiology and stress response.” *Physiologia Plantarum,* 2000, 108: 111-117.

[18] Cordero B, Otero A, Patino M, Arredondo BO, Fabregas J. 1996. Astaxanthin production from the green alga Haematococcus pluvialis with different stress conditions. Biotechnology Letters 18, 213–218.

[19] Demetriou G, Neonaki C, Navakoudis E, Kotzabasis K. “Salt stress impact on the molecular structure and function of the photosynthetic apparatus: the protective role of polyamines.” *Biochimica et Biophysica Acta*, 2007, 1767, 272–280.

[20] Wahid A, Gelani S, Ashraf M, Foolad MR. “Heat tolerance in plants: an overview.” *Environ Exp Bot,* (2007), 61, 199–223.

[21] Allakhverdiev S, Kreslavski V, Klimov V, Los D, Carpentier R, Mohanty P. “Heat stress: an overview of molecular responses in photosynthesis.” *Photosynth Res*, 2008, 98, 541-550.

[22] Berry JA, and Björkman O. “Photosynthetic response and adaptation to temperature in higher plants.” *Annu Rev Plant Physiol,* 1980, 31, 491–543.

[23] Law R, and Crafts-Brandner SJ. “Inhibition and acclimation of photosynthesis to heat stress is closely correlated with activation of ribulose-1,5-bisphosphate carboxylase/oxygenase.” *Plant Physiol,* 1999, 120, 173–182.

[24] Gounaris K, Brain ARR, Quinn PJ, Williams WP. “Structural reorganization of chloroplast thylakoid membranes in response to heat stress.” *Biochim Biophys Acta,* 1984, 766, 198–208.

[25] Sharkey TD. “Effects of moderate heat stress on photosynthesis: importance of thylakoid reactions, rubisco deactivation, reactive oxygen species, and thermotolerance provided by isoprene.” *Plant Cell Environ*, 2005, 28, 269–277.

[26] Pastenes C, and Horton R. “Effect of high temperature on photosynthesis in beans.” *Plant Physiol*, 1996, 112, 1245–1251.

[27] Salvucci ME, and Crafts-Brandner SJ. “Relationship between the heat tolerance of photosynthesis and the thermal stability of Rubisco activase in plants from contrasting thermal environments.” *Plant Physiol*, 2004, 134, 1460–1470.

[28] Bascuñán-Godoy L, Sanhueza C, Cuba M, Zuñiga G, Corcuera L, Bravo L. “Cold-acclimation limits low temperature induced photoinhibition by promoting a higher photochemical quantum yield and a more effective PSII restoration in darkness in the Antarctic rather than the Andean ecotype of *Colobanthus quitensis* Kunt Bartl (Cariophyllaceae).” *BMC Plant Biology*, 2012, 12, 114.

[29] Maxwell DP, Falk S, Huner N. "Photosystem II excitation pressure and development of resistance to photoinhibition (I. light-harvesting complex II abundance and zeaxanthin content in *Chlorella vulgaris*)."*Plant Physiology* 1995, 107.3, 687-694.

[30] Gray G, Chauvin LP, Sarhan F, Huner N. “Cold Acclimation and Freezing Tolerance (A Complex Interaction of Light and Temperature).” *Plant Physiol.*, 1997, 114, 467-474.

[31] Smith B, Morrissey P, Guenther J, Nemson J, Harrison M, Allen J, Melis A. “Response of the Photosynthetic Apparatus in *Dunaliella salina* (Green Algae) to Irradiance Stress.” *Plant Physiol.*, 1990, 93, 1433-1440.

[32] Melis, A. “Dynamics of photosynthetic membrane composition and function.” *Biochim. Biophys. Acta,* 1991*,* 1058, 87–106.

[33] Mitra M, Kirst H, Dewez D, Melis A. “Modulation of the light-harvesting chlorophyll antenna size in Chlamydomonas reinhardtii by TLA1 gene over-expression and RNA interference.” *Phil. Trans. R. Soc. B*, 2012, 367, 3430-3443.

[34] Lemoine Y, and Schoefs B. “Secondary ketocarotenoid astaxanthin biosynthesis in algae: a multifunctional response to stress.” *Photosynth. Res.*, 2010, 106, 155-177.

[35] Alscher RG, Donahue J, Cramer C. "Reactive oxygen species and antioxidants: relationships in green cells." *Physiol. Plant.*, 1997, 100, 224-233.

[36] Yoshimura K, Miyao K, Gaber A, Takeda T, Kanaboshi H, Miyasaka H, Shigeoka S. "Enhancement of stress tolerance in transgenic tobacco plants overexpressing *Chlamydomonas* glutathione peroxidase in chloroplasts or cytosol." *The Plant Journal*, 2004, 37, 21-33.

[37] Yamada T, Onimatsu H, Van Etten J. "*Chlorella* Viruses." *Advances in Virus Research*, 2006, 66, 293-336.

[38] Meints R, Lee K, Burbank D, Van Etten, J. "Infection of a *chlorella*-like alga with the virus, PBCV-1: Ultrastructural studies." *Virology*, 1984, 138, 341–346.

[39] Balachandran S, Hurry V, Kelley S, Osmond C, Robinson S, Rohozinski J, Seaton G, Sims D. "Concepts of plant biotic stress. Some insights into the stress physiology of virus-infected plants, from the perspective of photosynthesis." *Physiol. Plant*, 1997, 100, 203-213.

[40] Rothschild L, and Mancinelli R. "Life in Extreme Environments." *Nature*, 2001, 409, 6823.

[41] Pick, U. "Enigmatic Microorganisms and Life in Extreme Environments." *Cellular Origin and Life in Extreme Habitats*, 1999, 1, 467–478.

[42] Palozza P, and Krinsky N. "Astaxanthin and canthaxanthin are potent antioxidants in a membrane model." *Arch Biochem Biophys,* 1992, 297, 291–295.

[43] Boussiba S, Bing W, Yuan JP, Zarka A, Chen F. "Changes in pigment profiles of *Haematococcus pluvialis* during response to environmental stress." *Biotechnol Lett,* 1999, 21, 601–604.

[44] Kerr J, Wyllie A, Currie A. "Apoptosis: a basic biological phenomenon with wide-ranging implications in tissue kinetics." *British Journal of Cancer*, 1972, 26, 239–257.

[45] Yordanova Z, Woltering E, Kapchina-Toteva V, Iakimova E. "Mastoparan-induced programmed cell death in the unicellular alga *Chlamydomonas reinhardtii*." *Annals of Botany*, 2013, 111, 191-205.

[46] Harris M, and Thompson C, "The role of the Bcl-2 family in the regulation of outer mitochondrial membrane permeability." *Cell Death Differ*, 2000, 7 (12), 1182–1191.

[47] Majors B, Betenbaugh M, Chiang G. “Links between metabolism and apoptosis in mammalian cells: Applications for anti-apoptosis engineering.” *Metabolic Engineering*, 2007, 9, 317-326.

[48] Merchant S, et al. “The Chlamydomonas Genome Reveals the Evolution of Key Animal and Plant Functions.” *Science*, 2007, 318, 5848, 245-250.

[49] Yamasaki T, Voshall A, Kim EJ, Moriyama E, Cerutti H, Ohama T. “Complementarity to a miRNA Seed Region Is Sufficient to Induce Moderate Repression of a Target Transcript in the Unicellular Green Alga *Chlamydomonas reinhardtii.*” *The Plant Journal,* 2013, 76, 1045-1056.

[50] Rosenberg J. “Overcoming Obstacles to Algal Biofuel Production: Species Selection & Genetic Engineering of Stress Tolerance.” *Transformation*, 2009.

[51] Gallie D. “Controlling gene expression in transgenics.” *Current Opinion in Plant Biology*, 1998, 1, 166-172.

[52] Allfrey V. “Post-synthetic modifications of histone structure: A mechanism for the control of chromosome structure by the modulation of histone-DNA interactions.” *Chromatin and Chromosome Structure*, 1977, Chapter 5, 167-191.

[53] Katan-Khaykovich Y, and Struhl K. “Dynamics of global histone acetylation and deacetylation in vivo: rapid restoration of normal histone acetylation status upon removal of activators and repressors.” *Genes & Development*, 2002, 16, 743-752.

[54] Torchia J, Glass C, Rosenfeld M. “Co-activators and co-repressors in the integration of transcriptional responses. *Curr. Opin. Cell Biol*, 1998, 10, 373-383.

[55] Chen H, Lin R, Xie W, Wilpitz D, Evans R. “Regulation of hormone-induced histone hyperacetylation and gene activation via acetylation of an acetylase.” *Cell*, 1999, 98, 675–686.

[56] Krebs J, Kuo M, Allis C, Peterson C. “Cell cycle-regulated histone acetylation required for expression of the yeast HO gene.” *Genes & Dev,* 1999, 13, 1412–1421.

[57] Vogelauer M, Wu J, Suka N, Grunstein M. “Global histone acetylation and deacetylation in yeast.” *Nature*, 2000, 408: 495–498.

[58] van Dijk K, Marley K, Jeong BR, Xu J, Hesson J, Cerny R, Waterborg J, Cerutti H. “Monomethyl Histone H3 Lysine 4 as an Epigenetic Mark for Silenced Euchromatin in Chlamydomonas.” *The Plant Cell*, 2005, 17, 2439-2453.

[59] Santos-Rosa H, Schneider R, Bannister A, Sherriff J, Bernstein B, Emre N, Schreiber S, Mellor J, Kouzarides T. “Active genes are tri-methylated at K4 of histone H3.” *Nature*, 2002, 419, 407–411.

[60] Tamaru H, Zhang X, McMillen D, Singh P, Nakayama J, Grewal S, Allis C, Cheng X, Selker E. "Trimethylated lysine 9 of histone H3 is a mark for DNA methylation in *Neurospora crassa*." *Nat. Genet*, 2003, 34, 75–79.

[61] Candido EPM, Reeves R, Davie J. "Sodium Butyrate inhibits histone deacetylation in cultured cells." *Cell*, 1978, 14, 105-113.

[62] Boulikas T. "Chromatin domains and prediction of MAR sequences." *Int. Rev. Cytol,* 1995, 162A, 279–388

[63] Wang TY, Han ZM, Chai YR, Zhang JH. "A mini review of MAR-binding proteins." *Mol. Biol. Rep,* 2010, 37, 3553-3560.

[64] Bode J, Benham C, Knopp A, Mielke C. "Transcriptional augmentation: modulation of gene expression by scaffold/matrix-attached regions (S/MAR elements)." *Crit. Rev. Eukaryot. Gene Expr*, 2000, 10, 73–90.

[65] Wang TY, Hou WH, Chai YR, Ji X, Wang JM, Xue LX. "Nuclear matrices and matrix attachment regions from green alga: *Dunaliella salina*." *Acta Genetica Sinica*, 2005, 32, 12, 1312-1318.

[66] Allen G, Spiker S, Thompson W. "Use of matrix attachment regions (MARs) to minimize transgene silencing." *Plant Molecular Biology*, 2000, 43, 361-376.

[67] Mlynárová L, Loonen A, Heldens J, Jansen R, Keizer P, Stiekema W, Nap J. "Reduced position effect in mature transgenic plants conferred by the chicken lysozyme matrix-associated region." *Plant Cell,* 1994, 6, 417–426.

[68] Allen G, Hall G, Michalowski S, Newman W, Spiker S, Weissinger A, Thompson W. "High-level transgene expression in plant cells: effects of a strong scaffold attachment region from tobacco." *Plant Cell*, 1996, 8, 899–913.

[69] Zhao T, Li G, Mi S, Li S, Hannon G, Wang XJ, Qi Y. "A complex system of small RNAs in the unicellular green alga *Chlamydomonas reinhardtii.*" *Genes & Development*, 2007, 21, 1190-1203.

[70] Schroda M. "RNA silencing in Chlamydomonas: Mechanisms and tools." *Curr. Genet*, 2006, 49, 69–84.

[71] Ibrahim F, Rymarquis L, Kim E, Becker J, Balassa E, Green P, Cerutti H. "Uridylation of mature miRNAs and siRNAs by the MUT68 nucleotidyltransferase promotes their degradation in *Chlamydomonas*." *Proc Natl Acad Sci USA,* 2010, 107, 3906-3911.

[72] Rasala B, Lee P, Shen Z, Briggs S, Mendez M, Mayfield S. "Robust Expression and Secretion of Xylanase1 in *Chlamydomonas reinhardtii* by Fusion to a Selection Gene and Processing with the FMDV 2A Peptide." *PLoS ONE*, 2012, 7, 8.

[73] Halpin C. "Gene stacking in transgenic plants–the challenge for 21st century plant biotechnology." *Plant Biotechnol J,* 2005, 3, 141–155.

[74] Luke G, Escuin H, De Felipe P, Ryan M. "2A to the fore - research, technology and applications." *Biotechnol Genet Eng Rev,* 2010, 26, 223–260.

[75] Rasala B, Barrera D, Ng J, Plucinak T, Rosenberg J, Weeks D, Oyler G, Peterson T, Haerizadeh F, Mayfield S. "Expanding the spectral palette of fluorescent proteins for the green microalga *Chlamydomonas reinhardtii.*" *The Plant Journal*, 2013, 74, 545-556.

[76] Henley W, Litaker RW, Novoveská L, Duke C, Quemada H, Sayre R. "Initial risk assessment of genetically modified (GM) microalgae for commodity-scale biofuel cultivation." *Algal Research*, 2013, 2, 66-77.

[77] Allnutt FCT, Postier B, Sayre R, Coury D, Kumar A, Swanson A, Abad M, Perrine Z. "BIOSECURE GENETICALLY MODIFIED ALGAE" United States Patent Application Publication. Pub. No. US 2013/0109098 A1.

[78] Faruq J. "Characterizing the robustness of a stress tolerant transgenic algae and metabolic flux modeling for commercial productivity." 2011.

[79] Fischer B, Krieger-Liszkay A, Eggen R. "Photosensitizers Neutral Red (Type I) and Rose Bengal (Type II) Cause Light-Dependent Toxicity in *Chlamydomonas reinhardtii* and Induce the Gpxh Gene via Increased Singlet Oxygen Formation." *Environ. Sci. Technol,* 2004, 38, 6307-6313.

Appendix A – Stress Adaptability Data

UTEX 2244	Time	0	% Viability	6	% Viability	18	% Viability	30	% Viability	**42**	**% Viability**	43	% Viability	54	% Viability	66	% Viability	78	% Viability
stress at 42hrs																			
	Control	0.2	100.0	0.0771	99.71	0.149	99.70	0.781	99.80	1.33	99.10	1.19	99.80	3.92	100.00	13.3	100.00	19.5	99.90
		0.2		0.0875	99.43	0.153	99.80	0.761	99.90	1.16	99.40	1.21	99.70	3.68	100.00	13.7	100.00	17.3	100.00
		0.2		0.0821	98.99	0.153	99.80	0.724	99.90	1.13	99.40	1.17	99.20	3.59	99.90	13.2	100.00	18.9	99.90
	Average			0.082	99.38	0.152	99.77	0.755	99.87	1.21	99.30	1.19	99.57	3.73	99.97	13.4	100.00	18.57	99.93
	Std Dev.	0		0.005		0.002		0.029		0.108		0.020		0.171		0.265		1.137	
	Std Error	0		0.003		0.001		0.017		0.062		0.012		0.098		0.153		0.657	
	2uM RB	0.2	100.0	0.0764	100.00	0.149	99.60	0.739	99.90	0.982	99.60	1.36	94.10	5.34	79.60	12.4	99.40	21.8	99.50
		0.2		0.0818	99.39	0.157	99.30	0.783	99.80	0.954	98.90	1.29	92.70	5.48	78.10	14	99.50	20.5	99.20
		0.2		0.0738	99.55	0.155	99.00	0.767	99.90	0.991	99.50	1.17	94.00	5.23	77.90	15.7	99.70	20.4	99.00
	Average			0.0773	99.65	0.154	99.30	0.763	99.87	0.976	99.33	1.27	93.60	5.35	78.53	14.03	99.53	20.9	99.23
	Std Dev.	0		0.004		0.004		0.022		0.019		0.096		0.125		1.650		0.781	
	Std Error	0		0.002		0.002		0.013		0.011		0.055		0.072		0.953		0.451	
	10uM RB	0.2	100.0	0.101	100.00	0.162	99.70	0.63	99.90	0.919	99.90	0.94	36.70	1.54	73.60	3.17	94.20	3.4	67.60
		0.2		0.0905	99.08	0.167	99.40	0.636	99.70	0.872	99.30	0.911	36.70	1.43	70.80	2.78	94.50	3.55	67.30
		0.2		0.104	99.36	0.16	99.70	0.653	99.70	0.966	99.90	0.894	38.10	1.59	71.40	2.97	92.60	3.7	66.50
	Average			0.0985	99.48	0.163	99.60	0.640	99.77	0.919	99.70	0.915	37.17	1.52	71.93	2.97	93.77	3.55	67.13
	Std Dev.	0		0.007		0.004		0.012		0.047		0.023		0.082		0.195		0.150	
	Std Error	0		0.004		0.002		0.007		0.027		0.013		0.047		0.113		0.087	
	Control	0.2	100.0	0.122	99.45	0.242	99.40	0.935	100.00	1.82	99.60	1.54	99.80	1.96	99.90	12.5	100.00	17.7	99.50
		0.2		0.117	99.43	0.242	98.90	0.923	99.70	2.79	99.60	1.52	99.70	2.15	100.00	12	99.90	19.4	99.90
		0.2		0.122	98.91	0.229	99.10	0.929	99.70	2.55	99.70	1.48	98.90	2.05	100.00	13.2	100.00	18.6	99.80
	Average			0.120	99.26	0.238	99.13	0.929	99.80	2.39	99.63	1.51	99.47	2.05	99.97	12.57	99.97	18.57	99.73
	Std Dev.	0		0.003		0.008		0.006		0.505		0.031		0.095		0.603		0.850	
	Std Error	0		0.002		0.004		0.003		0.292		0.018		0.055		0.348		0.491	
	150mM NaCl	0.2	100.0	0.0928	99.10	0.185	99.70	0.787	99.60	1.52	99.30	1.47	100.00	1.83	99.70	5.19	99.30	5.74	99.30
		0.2		0.0928	99.46	0.178	99.80	0.822	99.60	1.51	99.70	1.42	100.00	2.01	99.90	4.46	99.50	4.3	99.10
		0.2		0.0935	99.11	0.164	99.30	0.79	99.70	1.61	98.90	1.46	99.90	2.02	99.30	4.71	99.50	4.63	98.50
	Average			0.0930	99.22	0.176	99.60	0.800	99.63	1.55	99.30	1.45	99.97	1.95	99.63	4.79	99.43	4.89	98.97
	Std Dev.	0		0.000		0.011		0.019		0.055		0.026		0.107		0.371		0.754	
	Std Error	0		0.000		0.006		0.011		0.032		0.015		0.062		0.214		0.436	
	250mM NaCl	0.2	100.0	0.0827	98.80	0.181	99.70	0.749	99.70	1.34	99.80	2.38	99.20	2.08	78.90	1.12	77.20	0.985	91.40
		0.2		0.0876	98.86	0.171	99.70	0.678	99.70	1.26	99.90	2.29	99.40	2.1	77.90	0.85	76.70	0.58	86.23
		0.2		0.0889	99.44	0.164	99.40	0.673	99.90	1.19	99.30	2.6	98.80	2.04	78.30	0.78	77.50	0.842	89.81
	Average			0.0864	99.03	0.172	99.60	0.7	99.77	1.26	99.67	2.42	99.13	2.07	78.37	0.917	77.13	0.802	89.15
	Std Dev.	0		0.003		0.009		0.043		0.075		0.159		0.031		0.180		0.205	
	Std Error	0		0.002		0.005		0.025		0.043		0.092		0.018		0.104		0.119	

pBR9	Time	0	% Viability	18	% Viability	30	% Viability	42	% Viability	**54**	**% Viability**	55	% Viability	66	% Viability	78	% Viability	90	% Viability
Stress at 54hrs																			
	Control	0.2	100.0	0.105	67.00	0.436	96.30	0.53	92.90	1.01	91.70	1.01	89.80	0.52	59.90	1.35	56.00	0.176	33.40
		0.2		0.098	63.10	0.39	96.70	0.52	92.80	0.989	90.80	0.915	89.60	0.549	62.30	1.22	52.50	0.874	51.30
		0.2		0.0909	61.90	0.41	96.60	0.523	94.00	0.891	92.60	0.892	89.60	0.543	57.00	1.24	53.40	0.46	46.60
	Average			0.0980	64.00	0.412	96.53	0.524	93.23	0.963	91.70	0.939	89.67	0.537	59.73	1.27	53.97	0.503	43.77
	Std Dev.	0		0.007		0.023		0.005		0.064		0.063		0.015		0.070		0.351	
	Std Error	0		0.004		0.013		0.003		0.037		0.036		0.009		0.040		0.203	
	2uM RB	0.2	100.0	0.123	69.00	0.261	96.70	0.721	93.90	1.06	90.10	0.553	50.70	0.0667	5.60	0.237	10.30	0.304	24.60
		0.2		0.116	65.10	0.228	96.80	0.713	94.20	0.954	89.30	0.567	48.90	0.495	4.50	0.207	9.60	0.173	27.80
		0.2		0.114	65.10	0.223	97.20	0.692	93.50	1.01	90.00	0.554	49.70	0.619	5.40	0.27	12.60	0.305	28.40
	Average			0.118	66.40	0.237	96.90	0.709	93.87	1.01	89.80	0.558	49.77	0.394	5.17	0.238	10.83	0.261	26.93
	Std Dev.	0		0.005		0.021		0.015		0.053		0.008		0.290		0.032		0.076	
	Std Error	0		0.003		0.012		0.009		0.031		0.005		0.167		0.018		0.044	
	10uM RB	0.2	100.0	0.094	65.20	0.298	97.40	0.587	95.70	0.758	91.40	0.0188	1.80	0.00175	0.20	0.00612	0.40	0.00509	0.70
		0.2		0.101	64.90	0.285	96.10	0.604	94.40	0.748	93.10	0.0121	1.20	0.00273	0.30	0.00534	0.40	0.0171	1.30
		0.2		0.11	67.50	0.264	97.20	0.592	94.90	0.719	92.30	0.0094	0.70	0.00351	0.40	0.013	1.00	0.0264	1.30
	Average			0.102	65.87	0.282	96.90	0.594	95.00	0.742	92.27	0.0134	1.23	0.002663	0.30	0.008153	0.60	0.016197	1.10
	Std Dev.	0		0.008		0.017		0.009		0.020		0.005		0.001		0.004		0.011	
	Std Error	0		0.005		0.010		0.005		0.012		0.003		0.001		0.002		0.006	
	Control	0.2	100.0	0.133	69.40	0.137	98.50	0.351	96.00	0.804	94.90	0.581	95.40	0.396	54.30	0.901	56.90	0.148	51.50
		0.2		0.158	70.50	0.133	97.50	0.327	96.60	0.768	94.40	0.549	95.20	0.462	56.20	0.796	58.00	0.529	47.50
		0.2		0.146	65.70	0.133	96.00	0.325	95.50	0.696	94.50	0.511	94.50	0.436	54.00	0.774	54.50	0.517	49.50
	Average			0.146	68.53	0.134	97.33	0.334	96.03	0.756	94.60	0.547	95.03	0.431	54.83	0.824	56.47	0.398	49.50
	Std Dev.	0		0.013		0.002		0.014		0.055		0.035		0.033		0.068		0.217	
	Std Error	0		0.007		0.001		0.008		0.032		0.020		0.019		0.039		0.125	
	150mM NaCl	0.2	100.0	0.113	70.30	0.234	97.80	0.525	95.90	1.06	94.10	1.06	94.20	0.36	51.00	0.487	47.50	0.129	53.20
		0.2		0.119	69.00	0.207	96.50	0.47	94.30	1.02	93.90	0.958	93.00	0.393	51.70	0.525	49.10	0.218	49.80
		0.2		0.114	66.80	0.207	96.20	0.482	95.30	0.993	92.20	0.956	93.40	0.385	52.60	0.578	49.80	0.305	48.00
	Average			0.115	68.70	0.216	96.83	0.492	95.17	1.02	93.40	0.991	93.53	0.379	51.77	0.53	48.80	0.217	50.33
	Std Dev.	0		0.003		0.016		0.029		0.034		0.059		0.017		0.046		0.088	
	Std Error	0		0.002		0.009		0.017		0.019		0.034		0.010		0.026		0.051	
	250mM NaCl	0.2	100.0	0.113	69.90	0.236	96.90	0.685	94.90	0.804	92.30	1.01	88.50	0.217	29.00	0.233	30.70	0.022	30.90
		0.2		0.105	67.30	0.227	95.60	0.681	92.80	0.698	90.70	0.934	90.80	0.218	29.60	0.248	30.10	0.0807	32.90
		0.2		0.114	67.80	0.23	96.80	0.683	94.30	0.685	90.50	0.974	92.00	0.22	28.30	0.234	31.30	0.231	30.90
	Average			0.111	68.33	0.231	96.43	0.683	94.00	0.729	91.17	0.973	90.43	0.218	28.97	0.238	30.70	0.111	31.57
	Std Dev.	0		0.005		0.005		0.002		0.065		0.038		0.002		0.008		0.108	
	Std Error	0		0.003		0.003		0.001		0.038		0.022		0.001		0.005		0.062	

pBG	Time	0	% Viability	6	% Viability	18	% Viability	**30**	**% Viability**	31	% Viability	42	% Viability	54	% Viability	66	% Viability	78	% Viability
Stress at 30hrs																			
	Control	0.2	100.0	0.217	99.80	0.322	100.00	0.925	99.90	1.14	100.00	7.73	99.80	9.58	99.90	9.77	100.00	12.9	99.90
		0.2		0.222	99.90	0.313	99.90	0.883	100.00	0.998	99.90	7.28	100.00	10.3	100.00	9.29	99.90	13	99.90
		0.2		0.222	100.00	0.304	99.80	0.899	99.80	1.14	99.70	7.29	100.00	9.9	99.90	9.16	100.00	12.5	99.90
	Average			0.220	99.90	0.313	99.90	0.902	99.90	1.09	99.87	7.43	99.93	9.93	99.93	9.37	99.97	12.8	99.90
	Std Dev.	0		0.003		0.009		0.021		0.082		0.257		0.361		0.321		0.265	
	Std Error	0		0.002		0.005		0.012		0.047		0.148		0.208		0.186		0.153	
	2uM RB	0.2	100.0	0.216	100.00	0.224	99.90	0.692	99.90	1.12	86.40	6	99.20	10.5	98.50	9.37	93.40	14	97.30
		0.2		0.23	99.80	0.225	99.90	0.667	99.80	0.998	83.90	5.8	99.50	8.99	98.90	8.85	91.70	12.7	96.40
		0.2		0.22	99.90	0.228	99.90	0.68	99.90	0.992	83.00	5.39	99.30	8.36	98.40	9.11	89.60	12.9	95.70
	Average			0.222	99.90	0.226	99.90	0.680	99.87	1.04	84.43	5.73	99.33	9.28	98.60	9.11	91.57	13.2	96.47
	Std Dev.	0		0.007		0.002		0.013		0.072		0.311		1.100		0.260		0.700	
	Std Error	0		0.004		0.001		0.007		0.042		0.180		0.635		0.150		0.404	
	10uM RB	0.2	100.0	0.248	99.90	0.485	99.90	1.72	100.00	0.0585	2.80	2.3	79.50	2.08	71.60	1.97	56.50	4.7	55.30
		0.2		0.257	100.00	0.457	100.00	1.74	100.00	0.078	3.90	2.22	82.60	2.06	70.70	1.99	56.40	4.41	52.10
		0.2		0.233	99.90	0.44	99.80	1.74	100.00	0.102	4.80	2.46	83.10	2.02	73.90	2.27	58.30	4.3	52.10
	Average			0.246	99.93	0.461	99.90	1.73	100.00	0.0795	3.83	2.33	81.73	2.05	72.07	2.08	57.07	4.47	53.17
	Std Dev.	0		0.012		0.023		0.012		0.022		0.122		0.031		0.168		0.207	
	Std Error	0		0.007		0.013		0.007		0.013		0.071		0.018		0.097		0.119	
	Control	0.2	100.0	0.24	100.00	0.425	100.00	1.55	100.00	1.41	99.90	9.61	100.00	12.2	99.90	14.1	99.90	18.6	99.80
		0.2		0.24	99.80	0.434	99.90	1.54	100.00	1.28	99.80	9.12	100.00	11	99.80	13.9	99.60	16.8	99.90
		0.2		0.214	97.80	0.425	100.00	1.47	99.90	1.32	99.80	8.98	99.80	11.7	100.00	13.6	99.90	18.3	99.90
	Average			0.231	99.20	0.428	99.97	1.52	99.97	1.34	99.83	9.24	99.93	11.63	99.90	13.87	99.80	17.9	99.87
	Std Dev.	0		0.015		0.005		0.044		0.067		0.331		0.603		0.252		0.964	
	Std Error	0		0.009		0.003		0.025		0.038		0.191		0.348		0.145		0.557	
	150mM NaCl	0.2	100.0	0.204	99.90	0.476	99.80	0.829	100.00	1.67	99.80	2.17	99.60	2.39	99.50	2.34	99.60	3.82	99.30
		0.2		0.202	99.80	0.47	99.80	0.787	99.90	1.72	100.00	2.16	99.60	2.52	99.00	2.42	98.70	4.06	99.70
		0.2		0.209	99.80	0.469	99.90	0.846	100.00	1.76	100.00	2.01	99.60	2.38	99.50	2.58	99.60	3.74	99.00
	Average			0.205	99.83	0.472	99.83	0.821	99.97	1.72	99.93	2.11	99.60	2.43	99.33	2.45	99.30	3.87	99.33
	Std Dev.	0		0.004		0.004		0.030		0.045		0.090		0.078		0.122		0.167	
	Std Error	0		0.002		0.002		0.018		0.026		0.052		0.045		0.071		0.096	
	250mM NaCl	0.2	100.0	0.273	100.00	0.634	100.00	0.919	100.00	1.85	100.00	0.654	67.60	0.561	64.50	0.398	81.40	0.465	89.20
		0.2		0.249	100.00	0.336	99.70	0.833	99.90	1.94	100.00	0.648	68.10	0.495	63.70	0.325	80.30	0.456	87.80
		0.2		0.249	99.70	0.328	99.80	0.849	99.90	2.02	99.80	0.591	65.60	0.508	60.80	0.366	80.20	0.43	89.10
	Average			0.257	99.90	0.433	99.83	0.867	99.93	1.94	99.93	0.631	67.10	0.521	63.00	0.363	80.63	0.450	88.70
	Std Dev.	0		0.014		0.174		0.046		0.085		0.035		0.035		0.037		0.018	
	Std Error	0		0.008		0.101		0.026		0.049		0.020		0.020		0.021		0.010	